ARTICLE IN PRESS

Swarm and Evolutionary Computation xxx (xxxx) 100511

Contents lists available at ScienceDirect

Swarm and Evolutionary Computation

journal homepage: www.elsevier.com/locate/swevo

# ESOEA: Ensemble of single objective evolutionary algorithms for many-objective optimization

Monalisa Pal *, Sanghamitra Bandyopadhyay

*Machine Intelligence Unit, Indian Statistical Institute, 203, Barrackpore Trunk Road, Kolkata, 700108, India*

ARTICLE INFO

*Keywords:*
Many-objective evolutionary algorithms
Differential evolution
Pareto-optimality
Non-dominated solutions
DTLZ, WFG, IMB and CEC 2009 competition test problems

ABSTRACT

Inspired by the success of decomposition based evolutionary algorithms and the necessary search for a versatile many-objective optimization algorithm which is adaptive to several kinds of characteristics of the search space, the proposed work presents an adaptive framework which addresses many-objective optimization problems by using an ensemble of single objective evolutionary algorithms (ESOEA). It adopts a reference-direction based approach to decompose the population, followed by scalarization to transform the many-objective problem into several single objective sub-problems which further enhances the selection pressure. Additionally, with a feedback strategy, ESOEA explores the directions along difficult regions and thus, improving the search capabilities along those directions. For experimental validation, ESOEA is integrated with an adaptive Differential Evolution and experimented on several benchmark problems from the DTLZ, WFG, IMB and CEC 2009 competition test suites. To assess the efficacy of ESOEA, the performance is noted in terms of convergence metric, inverted generational distance, and hypervolume indicator, and is compared with numerous other multi- and/or many-objective evolutionary algorithms. For a few test cases, the resulting Pareto-fronts are also visualized which help in the further analysis of the results and in establishing the robustness of ESOEA.

## 1. Introduction

Many-objective optimization (MaOO) algorithms are designed for addressing those optimization problems which have more than three conflicting optimization criteria (objectives) [1,2]. Formally, a box-constrained multi-objective optimization (MOO) problem [3] (Eq. (1)) maps $N$ decision variables ($X = [x_1, \dots, x_N]$) to $M$ objective values ($F(X)$), which are to be optimized. Thus, a MaOO problem belongs to the sub-group of such MOO problems with $M \geq 4$.

$$\begin{aligned} &\text{Minimize } F(X) = [f_1(X), f_2(X), \dots, f_M(X)] \\ &\quad \text{where, } X \in \Re^N, F(X) : \Omega \mapsto \Re^M \\ &\quad \text{and } \Omega : x_j^L \leq x_j \leq x_j^U, \forall j = 1, 2, \dots, N \end{aligned} \tag{1}$$

Unlike mathematical optimization algorithms, which can generate only one optimal solution in a single run, evolutionary algorithms (EAs) are popular due to their inherent capability to parallelly search for the optimal solution using a population of candidates [1,2,4,5] and also due to their ability to generate near-optimal solutions even for hard problems [3]. Such EAs for MOO and/or MaOO problems are widely applied across multiple domains [6–10] which uncover more practical challenges and thus, the search for better algorithms is afresh.

Two $M$-objective vectors are compared by Pareto-dominance relation where $X$ Pareto-dominates $Y$ by Eq. (2). The desired solution of a MOO problem is a set of multiple trade-offs among the several conflicting objectives which represents the state of Pareto-optimality (no solution can be improved in any objective without degrading any other objective) [1,2,5]. This optimal set of solution vectors and their corresponding objective vectors are called Pareto-optimal set and Pareto-front, respectively, and are estimated using the set of non-dominated solutions.

$$\begin{aligned} &X \prec Y \iff (f_i(X) \leq f_i(Y) \wedge f_j(X) < f_j(Y)), \\ &\forall i \in \{1, 2, \dots, M\}, \text{ and } \exists j \in \{1, 2, \dots, M\} \end{aligned} \tag{2}$$

Literature has an abundance of several MOO algorithms where second-generation non-dominated sorting genetic algorithm (NSGA-II) [11], strength Pareto EA 2 (SPEA2) [12] and second generation Pareto-envelop based selection algorithm (PESA-II) [13] are the distinguishable ones. However, when these algorithms are applied to MaOO problems, several issues appear [1,5,14,15]. These major challenges are: (i)

* Corresponding author.
*E-mail addresses:* monalisapal_r@isical.ac.in (M. Pal), sanghami@isical.ac.in (S. Bandyopadhyay).

https://doi.org/10.1016/j.swevo.2019.03.006
Received 1 March 2018; Received in revised form 9 March 2019; Accepted 9 March 2019
Available online XXX


Please cite this article as: M. Pal, S. Bandyopadhyay, ESOEA: Ensemble of single objective evolutionary algorithms for many-objective optimization, Swarm and Evolutionary Computation, https://doi.org/10.1016/j.swevo.2019.03.006

dominance resistance [16] i.e. the phenomena of saturation of population with non-dominated solutions which leads to decrease in selection pressure, (ii) curse of dimensionality i.e. requirement of more number of individuals to approximate the Pareto-front and to balance the trade-off between convergence and diversity, and (iii) visualization difficulties to validate the convergence and diversity of Pareto-fronts. Moreover, from a decision-maker's perspective, a good representation of Pareto-front is essential [15]. However, these representative characteristics are captured differently by various performance indicators [14]. To tackle these issues of applying EAs to MaOO problems, research studies are broadly categorized into four classes viz. Pareto-dominance based algorithms, indicator based algorithms, objective reduction based algorithms and decomposition based algorithms.

The first class involves modification of the Pareto-dominance relationship to enhance the selection pressure such as $\epsilon$-dominance [17], $\theta$-dominance [18], favour relation [19], fuzzy Pareto-dominance [20] and grid dominance [21]. A few such tailored Pareto-dominance based MaOO algorithms are grid dominance based EA (GrEA) [21], $\theta$-dominance based EA ($\theta$-DEA) [18] and knee point driven EA (KnEA) [22].

The second class involves algorithms which consider convergence and diversity indicators as selection criteria. Common indicator based algorithms are indicator based EA (IBEA) [23], S-metric selection based evolutionary multi-objective algorithm (SMS-EMOA) [24], generational distance and $\epsilon$-dominance based multi-objective EA (GDE-MOEA) [25], R2 indicator based many-objective meta-heuristic II (MOMBI-II) [26] and algorithm based on hypervolume estimation (HypE) [27]. Hypervolume indicator has gained immense attention due to its success, however, its computational complexity increases exponentially with the number of objectives. There has been some effort towards generalization hypervolume for MaOO problems such as by using Monte-Carlo simulation [27] or weakly Pareto-complaint Sharpe-Ratio indicator [28].

The third class involves algorithms which transform a MaOO problem into a simpler problem by reducing the number of objectives so that the induced Pareto-optimal set remains invariant [10,14]. Hence, it combines dimensionality reduction techniques like Principal component analysis [29], clustering based approaches [10,14], feature selection [30,31], and so on, in a framework, to deal with MaOO problems. The intuition behind such approaches is to reduce the problem complexities such that MaOO problems could efficiently be handled by existing MOO algorithms. However, investigating the optimal objective subset is tedious albeit essential for every new problem.

The fourth class involves decomposition based algorithms. Such algorithms decompose a MOO or MaOO problem into multiple scalar optimization subproblems which collaborate with each other to be optimized. Some notable algorithms of this class are decomposition based multi-objective EA (MOEA/D) [32], dynamic weight based EA (EDWA) [33], multiple single objective Pareto sampling algorithm-II (MSOPS-II) [34] and multi-objective genetic local search (MOGLS) [35]. Two recent and successful approaches of this class are MOEA/D-M2M (transforms MOO problem into simpler MOO subproblems) [36,37] and third generation NSGA or NSGA-III (uses reference points to enhance convergence and diversity) [38].

Among these classes of algorithms, decomposition based algorithms have shown promising performance in addressing MaOO problems. Moreover, neither such approaches face dominance resistance in high dimensional objective space like Pareto-dominance based approaches nor such approaches require the extreme computational effort for hypervolume evaluation. However, MOEA/D variants suffer from the following shortcomings:

1. Replacement of an old solution by a new solution is dictated by scalarization function values [32,39], which may miss some search regions, leading to severe loss of population diversity.
2. Setting the weight vectors and the scalarization function is problem specific [32,39] which can be a daunting task for every new kind of a problem.
3. Performance of these algorithms strongly depends on whether the distribution of reference vectors is consistent with the shape of Pareto-front [40].

Hence, these algorithms have limited adaptive capabilities to modify their exploration tendencies as per problem requirement. Earlier studies on adaptability report results only for 2 or 3-objective problems [41,42]. Even the work in Ref. [43], which presents an adaptive MaOO framework, has reported its performance for up to 8-objective problems. Hence, their extensibility for problems with a large number of objectives is yet to be studied.

The standard reproduction operators of Genetic Algorithm (GA) [44] or Differential Evolution (DE) [45,46] are essentially designed for candidate-wise operation i.e. for single-objective EAs. In contrast, the solution of MOO problems is characterized by a set of candidate solutions. Yet most of the existing MOO and/or MaOO algorithms directly adopt these vector-wise (instead of set-wise) reproduction operators for yielding the next generation, without proper justification, as pointed out in Ref. [42]. Moreover, the existing algorithms are specifically tailored for particular types (difficulties and shape) of Pareto-fronts [40,47]. In practice, the type of Pareto-front or the difficulties in the objective space are unknown. Hence, the literature of MOO algorithms still lacks a robust algorithm with adaptive search-ability. Motivated by these requirements, the authors propose an adaptive framework for dealing with MaOO problems using an ensemble of single objective evolutionary algorithms (ESOEA) whose major contributions are as follows:

1. It uses randomized candidate association for population decomposition which is much faster than the exhaustive candidate association used in several existing approaches [36,38,48].
2. It uses multiple single objective evolutionary algorithms (SOEA), similar to decomposition based approaches, such that the selection pressure is maintained. The use of SOEA justifies the use of candidate-wise reproduction operators. Moreover, as decomposition based approaches concentrate on each sub-region, unlike the existing approaches, the proposed approach uses a SOEA with adaptive hyper-parameters such that sub-region specific problem characteristic could be efficiently addressed.
3. It uses a regulated elitism scheme where only a fraction of rank-one solutions is inherited by the next parent population and thus, it avoids the saturation problem of MaOO algorithm for a high number of objectives. Moreover, it performs elitist selection only after periodic intervals. Elitist selection involves executing the non-dominated sorting, which is the most computationally expensive step when performed only at periodic intervals lead to considerable saving in running time of the algorithm.
4. It adaptively allocates candidate to optimizers on the basis of contribution to forming the parent population for the next generation. Thus, it boosts those sub-optimizers which performs poorly.

To the best of the authors' knowledge, a MaOO algorithm (viz. ESOEA) focusing on so many aspects has not been developed until now and these features highlight the novelty of the proposed work.

Rest of the paper is structured as follows. Background information on related existing approaches is presented in Section 2. The general outline of the proposed framework is described in Section 3. Performance analysis through various experiments is performed in Section 4 while highlighting the importance of the different modules composing the proposed framework. Finally, Section 5 draws the conclusion while mentioning the future research scope of the proposed work.

## 2. Background information

In this section, some basic concepts are presented about the scalarization functions which are commonly used in the decomposition methods. Then, the general mechanisms of existing approaches, which are related to this paper, are briefly described.

### 2.1. Scalarization methods

There are several scalarization approaches in the literature which obtain a scalar fitness value corresponding to an objective vector of a MOO problem [1,2,5]. Among these, the most commonly used functions [15,48] are weighted sum, Tchebycheff and boundary intersection functions. In Ref. [49], the normal-boundary intersection (NBI) method has been proposed which considers a vector for scalar transformation with an equality constraint. This approach has later been modified as an unconstrained variant by using a penalty parameter ($\theta$) which is called as the penalty-based boundary intersection (PBI) approach [32,49]. This work adopts the PBI based approach due to its remarkable performance for MaOO problems [15,32,49]. Formally, the scalar optimization problem obtained by transformation with respect to weight/reference vector ($W$), is given by Eq. (3) where $f^{min} = [f_1^{min}, f_2^{min}, \ldots, f_M^{min}]$ with $f_i^{min} = min_{X\in\Omega} f_i(X)$.

$$\begin{aligned}
&\text{Minimize } F_{pbi}(X \mid W, f_{min}) = d1 + \theta \times d2 \\
&\text{where, } X \in \Omega,\ \theta \geq 0,\ d1 = \frac{\left\| \left(F(X) - f^{min}\right)^T W \right\|}{\|W\|} \\
&\text{and } d2 = \left\| F(X) - \left(f^{min} + d1 \frac{W}{\|W\|}\right) \right\|
\end{aligned} \tag{3}$$

In PBI function (Eq. (3)), $d1$ describes the convergence of the projection of the objective vector along the weight vector and $d2$ denotes the perpendicular distance from the objective vector to the weight vector. Hence, $d2$ indicates the diversity of the solution set. The penalty parameter ($\theta$) balances the degree of convergence and diversity such that $F(X)$ moves to the boundary of $F_{pbi}$ along each of the weight vectors.

### 2.2. Related works

To alleviate one or more of the drawbacks of decomposition based approaches, only recently, MOO literature has seen some novel reference point based approaches such as adaptive-NSGA-III (or A-NSGA-III) [50], MOEA/D-M2M [36,37], dominance and decomposition based multi-objective EA (MOEA/DD) [15], reference vector guided EA (RVEA) [48] and adaptive reference point based multi-objective EA (AR-MOEA) [47]. Different literature uses different terminologies to mean reference point, reference vector, direction vector or weight vector. In this work, all these terminologies are synonymous. It should be noted that the purpose of weight vectors have been different in different algorithms, like in MOEA/D-M2M and RVEA, weight vectors assist in specifying subpopulations, in MOEA/DD and NSGA-III, weight vectors assist in local density estimation, in AR-MOEA, adapted weight vectors assist in evaluation of a scalar indicator to address the Pareto-front shape while guiding the selection.

MOEA/D-M2M [36,37] decomposes a MOO problem into multiple simpler MOO problems each constrained to an acute angle based neighborhood with respect to reference vectors. At each generation, reproduction of candidates occurs within each subpopulation. These subpopulations are then merged and re-allocated to different subproblems of fixed size. This periodic merging helps it to achieve a better global diversity compared to existing MOEA/D variants.

MOEA/DD [15] takes the advantages of dominance as well as decomposition to balance between convergence and diversity. It has a similar framework like MOEA/D, however, some modules are essentially different in operation. It uses neighborhood-based parent selection for mating, the steady-state selection scheme to update population and an update scheme which is governed by Pareto-dominance, niche count and scalarization function, sequentially.

RVEA [48] is a decomposition based algorithm similar to MOEA/D-M2M where the reference vector guides the selection process based on a novel scalarization function viz. angle-penalized distance (APD). RVEA also proposes reference vector adaptation and regeneration strategies to tackle scaled MaOO problems and MaOO problems with irregular Pareto-fronts, respectively.

Another strategy to address different shape and distribution of the Pareto-fronts is by reference point adaptation methods. Some reference point adaptation strategies modify the location of the reference points based on the distribution of solutions in the current population such as in A-NSGA-III [50] and RVEA∗ [48] whereas other strategies are based on the solution distribution in an external archive such as in $pa\lambda$-MOEA/D [51] and MOEA/D-AWA [52]. Roughly, the general steps of reference point adaptation involve deletion of reference points corresponding to empty niche or empty subspace or a region having sparsely located solutions, followed by adding reference points randomly or in a crowded region or in a hyperbox specified by the nadir and ideal points of the current population. However, these algorithms with reference point adaptation strategies perform better for MOO problems with irregular Pareto-fronts than those with regular Pareto-fronts due to perturbation of initial uniform distribution of reference points [47].

Another notable recent approach is AR-MOEA [47] which is motivated to evolve an external archive, conforming to the Pareto-front shape. It performs selection using an indicator, called inverted generational distance with non-contributing solution (IGD-NS), with respect to the external archive, along with a reference point adaptation strategy to tackle those MaOO problems which have different types (regular and irregular shapes) of Pareto-fronts. It involves four sets of solutions viz. the evolving population at each generation, the initial set of reference points, the external archive and the set of adapted reference points. The adapted reference point set borrows those reference points from the initial reference set which are closest to contributing solutions and those solutions from the external archive which have maximum angles to former points. Thus, the adapted set reflects both the initial uniform distribution and the shape of the Pareto-front.

Encompassing all the drawbacks of decomposition based approaches mentioned in Section 1, the contemporary MOO and/or MaOO algorithms have shown excellent performance. However, these algorithms suffer from the following disadvantages:

1. Although MOEA/D-M2M has drawn considerable attention, it requires substantial computational effort to be extended for MaOO problems. Moreover, as it has been designed for problems with imbalance difficulties or variable linkage difficulties [37], its extension for problems with irregular Pareto-front has not been investigated.
2. With a high number of objectives ($M > 10$), the non-dominated set of solutions span almost the entire population [10,20]. However, in several of these algorithms viz. MOEA/D-M2M [36], NSGA-III [38], and AR-MOEA [47], the population of the next generation inherits the entire rank-one solutions. Thus, high-ranked diverse solutions have very little survival chances.
3. Some of these algorithms viz. NSGA-III [38], RVEA [48] and MOEA/D-M2M [36] associate candidates with weight vectors during the selection step. This association requires distance or angle between all objective vectors and weight vectors. Its evaluation becomes costlier when the location of reference vectors are not constant such as in RVEA∗ [48] or A-NSGA-III [50] where reference vectors are adapted as per problem characteristics.

Thus, the need of the hour is a MaOO algorithm which exhibits robust performance with regards to various problem types, reducing the effect of the above drawbacks.

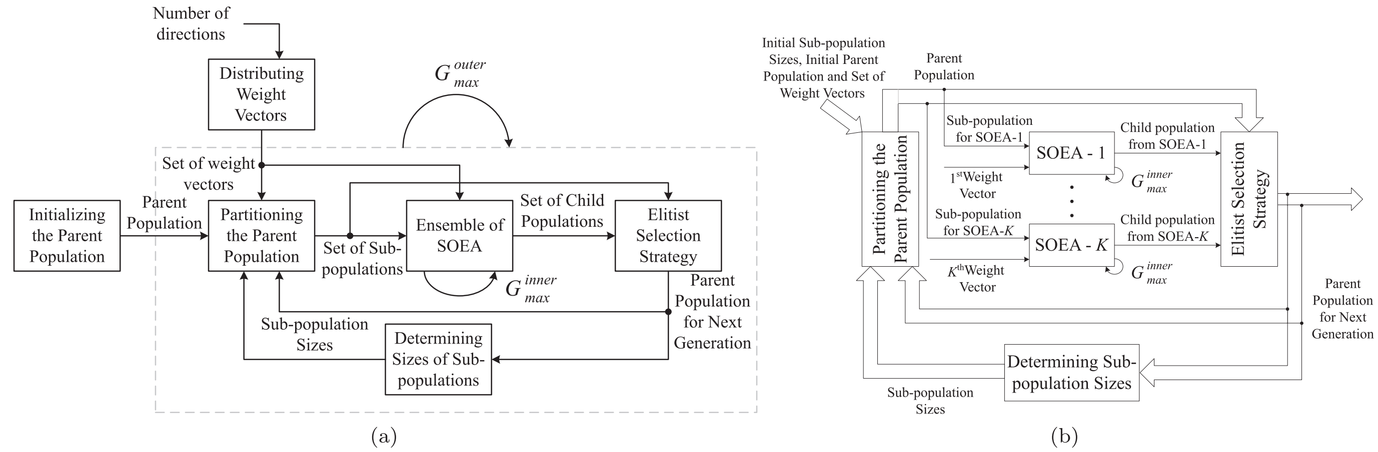


**Fig. 1.** (a) Overall framework showing the information flow among different building blocks, (b) Elaborating the central loop of Ensemble of Single Objective Evolutionary Algorithms (ESOEA).

## 3. The proposed algorithmic framework

This section describes several modules involved in building the entire framework for addressing multi- or many-objective optimization using multiple instances of single objective optimization algorithms. The overall framework is outlined in Fig. 1a, whose central loop (marked by the dashed rectangle) is elaborately described in Fig. 1b. The constituent units are subsequently discussed.

### 3.1. Distributing weight vectors

Distribution of a number of weight vectors, in the objective space, constitute the first step of the proposed approach. It is essential that the weight vectors are uniformly spread out in the objective space. Moreover, only the final distribution of weight vectors influences the rest of the algorithmic framework, and hence, this uniform weight initialization can be performed offline i.e. the weight initialization problem can be solved before using the proposed approach to solve a MaOO problem. For a fair comparison, weight initialization is performed using the two-layered systematic approach as described in NSGA-III [38] and MOEA/DD [15]. This ensures that a reasonable number of weights ($K$) are uniformly initialized in the objective space such that a certain number of direction vectors ($K_1$) are defined along the boundary of an $(M-1)$-dimensional unit hyperplane with $p_1$ divisions along each objective and remaining vectors ($K_2$) are in the non-boundary region of the hyperplane with $p_2$ divisions along each objective. These weight vectors are stored in a matrix ($X_W$) of order $K \times M$ as shown in Eq. (4).

$$X_W = [W_1, W_2, \dots, W_K]^T \text{where } W_i = [w_{i1}, \dots, w_{iM}]$$
$$\text{and } K = K_1 + K_2 = \binom{M+p_1-1}{p_1} + \binom{M+p_2-1}{p_2} \tag{4}$$

### 3.2. Initializing the parent population

Similar to most of the evolutionary algorithms [3,14], the initial population of $NP$ candidate solutions are randomly initialized, uniformly within the boundaries of the search space ($\Omega$), as shown in Eq. (5) where $rand(0,1)$ indicates a random real number between 0 and 1.

$$X_{i,G=1} = \left[x_{i1,G=1}, x_{i2,G=1}, \dots, x_{iN,G=1}\right]$$
$$\text{where, } x_{ij,G=1} = x_j^L + rand(0,1) \times \left(x_j^U - x_j^L\right), \tag{5}$$
$$\forall i = 1, \dots, NP, \forall j = 1, \dots, N$$

### 3.3. Partitioning the parent population (decomposition)

Prior to partitioning the parent population, objective scaling is attempted such that the scales of the objective function have minimal influence on the other modules. Thus, an array of reference objective value is obtained from the parent population (as shown in Eq. (6)) which is used for objective scaling. This array of reference objective values is updated in every generation of the central loop from the new parent population, prior to partitioning the parent population.

Objective scaling is performed on the objective values of every candidate ($X_i$) of the parent population (prior to partitioning the parent population using updated reference objective values) as well as on every candidate ($XC_i^k$) of all the child sub-populations (within every instance of the ensemble of single objective optimizers) for every generation. Thus, during elitist selection step, the set of objective values corresponding to every candidate of the merged population remain scaled with respect to the same set of reference objective values and thus, does not influence the selection of candidates.

For generation $G$, the objective scaling for any of the $i$th candidate of any population (parent or child) occurs as shown in Eq. (7).

$$F_G^r = [f_{1,G}^r, f_{2,G}^r, \dots, f_{M,G}^r]$$
$$\text{where, } f_{j,G}^r = \max_{i=1}^{NP} f_j(X_{i,G}), \forall j = 1, \dots, M \tag{6}$$

$$F^s(Y_i) = \left[\frac{f_1(Y_i)}{f_{1,G}^r}, \frac{f_2(Y_i)}{f_{2,G}^r}, \dots, \frac{f_M(Y_i)}{f_{M,G}^r}\right]$$
$$\text{where, } Y_i = X_{i,G} \text{ or } Y_i = XC_{i,G}^k \tag{7}$$

Now, considering there are $K$ directions/divisions, population decomposition aims to select the candidates of the $k$th sub-population ($X^k$) such that their scaled corresponding objectives ($F^s(X^k)$) are close to its associated direction ($\overrightarrow{OW_k}$).

#### 3.3.1. Usual approach

This is usually achieved by associating each candidate to its nearest neighboring direction vector using perpendicular distance from objective vector to direction vector [15,38] (as shown in Fig. 2a) or using the acute angle between these two vectors [36,48]. In each generation, the required time complexity for such an exhaustive association is $\mathcal{O}(NP \cdot M \cdot K)$. An exhaustive association also helps in elimination of candidates during elitist selection. When $NP$ is chosen approximately equal to $K$ [38], the time complexity becomes $\mathcal{O}(M \cdot (NP)^2)$.

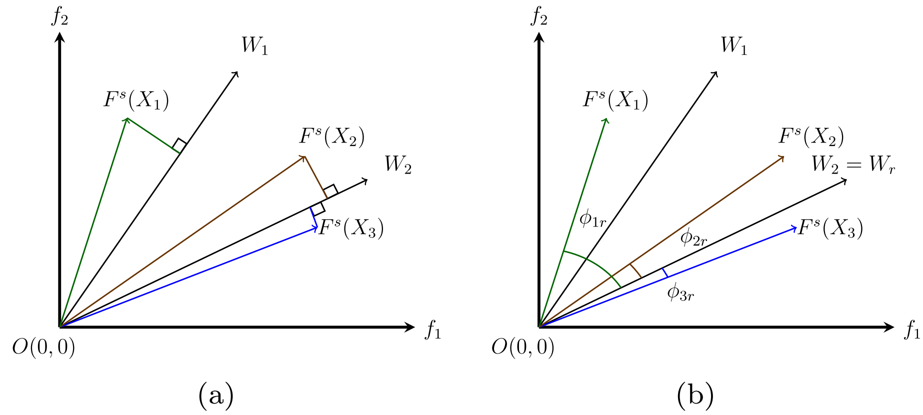


**Fig. 2.** Candidate association for population decomposition: (a) Usual approach of exhaustive association, (b) Proposed approach of randomized association.

### *3.3.2. Proposed approach*

In the proposed method, a randomized association is adopted instead of exhaustive association. The pseudo-code for this randomized population decomposition is given in Algorithm 1 and its example is illustrated in Fig. 2b. The algorithm starts with selecting a random direction called $\overrightarrow{OW_r}$ (line 2), followed by sorting of all the weight vectors based on Euclidean distance $D(.)$ from $W_r$ (line 3) and sorting of all the candidate solutions based on the angle $\phi$ (defined by Eq. (9)) between their scaled objective vectors and $W_r$ (line 4). To form the sub-populations, the for-loop (line 5 to 10) assigns portions of the sorted population to the sorted directions, in sequential order. For the initial generation (generations for central loop are labeled as $G$), the size of all sub-populations is given by Eq. (8), where *round*(.) helps to round sub-population size to nearest integer using round-half-to-even method (the default rounding mode used in IEEE 754 floating point computations [53]). This initialization indicates that all $K$ directions are equally likely to be searched. For other generations ($G \neq 1$), determination of the size of the sub-population is discussed later in Section 3.6.

$$\left|X^k_{G=1}\right| = \begin{cases} round(NP/K), & \forall k \neq K \\ NP - \sum\limits_{k=1}^{K-1} \left|X^k_{G=1}\right| & \text{when } k = K \end{cases} \tag{8}$$

$$\phi_{jr} = \phi\left(\overrightarrow{OF^s(X_j)}, \overrightarrow{OW_r}\right) = \arccos\left(\frac{\overrightarrow{OF^s(X_j)} \cdot \overrightarrow{OW_r}}{\left\|\overrightarrow{OF^s(X_j)}\right\| \times \left\|\overrightarrow{OW_r}\right\|}\right) \tag{9}$$

The dominant steps of Algorithm 1 are the sorting steps (in line 3 and 4) which use the Quick Sort [54] algorithm with $\mathcal{O}\left(\mathcal{N} \cdot log_2\mathcal{N}\right)$ complexity for sorting $\mathcal{N}$ entries. Hence, the time complexity of such randomized candidate association for population decomposition is $\mathcal{O}\left(M \cdot K \cdot \log_2(M \cdot K) + M \cdot NP \cdot \log_2(M \cdot NP)\right)$ which becomes equal to $\mathcal{O}\left(M \cdot NP \cdot \log_2(M \cdot NP)\right)$ when $NP$ is chosen approximately equal to $K$. The time complexities of the usual and the proposed approach are plotted as functions of $NP$ and $M$ in Fig. 3 which shows the dashed lines are lower than the dotted lines implying the proposed approach has much less time complexity for standard values of $M$ and $NP$ from Refs. [3,10,14,38].

After population decomposition, the sub-populations are used as the initial population of each instance of the ensemble of optimizers.

### *3.4. Ensemble of single objective optimizers*

In this module, $K$ instances of a single objective evolutionary algorithm (SOEA) are used to evolve each sub-population for a small, predetermined number of generations ($G^{inner}_{max}$) as shown in Fig. 1b. Here, reproduction operators of the SOEA are used on the sub-population produce new child sub-population. However, during the selection stage

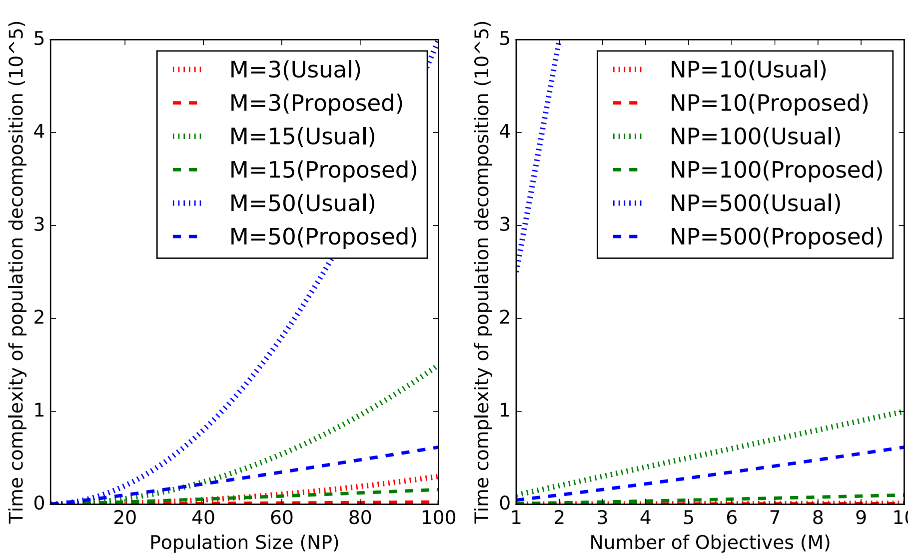


**Fig. 3.** Comparison of time complexities of the usual and the proposed population decomposition strategies.

**Algorithm 1** Procedure for Partitioning the Population.
**Input:** $F^s(X)$: Scaled fitness of entire population; $\{|X^k|\}$: Set of sub-population sizes; $K$: Number of direction vectors; $\{\overrightarrow{OW_k}\}$: Set of direction vectors
**Output:** $\{X^k\}$: Candidates for each of the $K$ sub-populations

1: **procedure** CandAssoc$\{\overrightarrow{OW_k}\}$, $F^s(X)$, $\{|X^k|\}$, $K$
2: Choose $\overrightarrow{OW_r}$, where, $r = random\_integer(1, K)$
3: $ind_W = \arg\text{sort}_{i=1}^{K}\left(\{D(W_r, W_i)\}, ascend\right)$
4: $ind_X = \arg\text{sort}_{j=1}^{NP}\left(\phi\left(\overrightarrow{OF^s(X_j)}, \overrightarrow{OW_r}\right), ascend\right)$ where, $\phi(.)$ is given by Eq. (9)
5: **for** $k = 1$ to $K$ (for each sub-population) **do**
6: Let $X^{temp}$ be the candidates corresponding to $ind_{temp}$, where $ind_{temp}$ is the set of first $\left|X^k_{G+1}\right|$ indices from $ind_X$
7: Assign: $X^{ind_W(k)} = X^{temp}$
8: $ind_X = \{ind_X \backslash ind_{temp}\}$
9: $ind_W = \{ind_W \backslash ind_W(k)\}$
10: **end for**
11: Return $\{X^k\}$
12: **end procedure**

of every $k$th optimizer, for conversion of a MaOO problem to a single objective optimization problem, the scalarization strategy of PBI (as shown in Eq. (10)) is considered.

$$F_W(X_i^k) = F_{pbi}(X_i^k | W_k, f_{\min}) \tag{10}$$

At the end of $G_{\max}^{inner}$ generations, every $k$th SOEA generates the child sub-population $XC_G^k$. The parent population ($X_G$) and the set of child sub-populations ($\{XC_G^k\}$) undergo elitist selection to yield the parent population for the next generation of the central loop ($X_{G+1}$).

### 3.5. Elitist selection strategy

Elitism [1,2] is a strategy which helps to retain the parent candidates that remain non-dominated even with respect to the newly generated child candidates. The work in Ref. [55] states that for any multi-objective evolutionary algorithms (MOEA), elitism is necessary in order to guarantee convergence.

#### 3.5.1. Usual approach

The usual approach to implement elitism has the following attributes:

1. Non-dominated sorting [10,11,14] is performed to rank the candidates, followed by the selection of the low-ranked sets of candidates until the parent population for the next generation is fully populated i.e. until the number of candidates ($|X_{G+1}|$) becomes equal to $NP$.
2. For generation $G$, the non-dominated set of candidates with respect to the merged population, i.e., $X_G \cup \left(\cup_{k=1}^{K} XC_G^k\right)$, forms the rank-one solutions ($R_{1,G}$) [11,14]. For any rank $p$ (with $p > 1$), the rank-$p$ solutions are given by Eq. (11) where $ndset(.)$ refers to the non-dominated set of the argument. The concept of rank-one solutions ($R_{1,G}$) is very crucial as it forms the resulting Pareto-optimal-set when the $M$-objective optimization terminates [11,14].
3. Since the selection occurs with one set of ranked candidates at a time, often a fraction of the last set is required to complete the set of parent population.
4. Sorting of the last required set of candidates is based on a secondary diversity preserving metric which assists in elimination of those undesirable candidates that map to densely populated regions of the objective space [1,2]. One such diversity indicator is the crowding distance (given by Eq. (12)), used in NSGA-II [11], MOEA/D-M2M [36], $\alpha$-DEMO [10], DECOR [14] and many other MaOO algorithms. It indicates densely crowded regions [14] where neighboring candidates form a hyper-rectangle having a small perimeter (Eq. (12)). Some other secondary selection criteria, in decomposition based MaOO algorithms, are niche count in NSGA-III [38], APD in RVEA [48] and IGD-NS in AR-MOEA [47]. Sometimes, a tie in the secondary selection criterion is broken using a tertiary criterion like niche count followed by PBI in MOEA/DD [15].

$$R_{p,G} = ndset\left(\left(X_G \cup \left(\cup_{k=1}^{K} XC_G^k\right)\right) \setminus \left(\cup_{q=1}^{p-1} R_{q,G}\right)\right) \tag{11}$$

$$CD(Y_i) = \sum_{j=1}^{M} CD(Y_i \mid f_j), \text{ where,}$$
$$CD(Y_i \mid f_j) = \begin{cases} 1000, & \text{if } f_j(Y_i) = f_j^{\max} \\ & \text{or } f_j(Y_i) = f_j^{\min} \\ \left|\dfrac{f_j(Y_{i+1}) - f_j(Y_{i-1})}{f_j^{\max} - f_j^{\min}}\right|, & \text{otherwise} \end{cases} \tag{12}$$

with $\{Y_{i-1}, Y_i, Y_{i+1}\} \subseteq R_{q,G}$ and $R_{q,G}$ is sorted by $f_j$

However, a major disadvantage arises when this approach of elitist selection is used for 10 or higher objective optimization problems [10,20]. This is because the merged population gets saturated with non-dominated solutions (i.e. $R_{1,G}$) and thus, there are always $NP$ or more number of candidates from $R_{1,G}$ to form $X_{G+1}$. Hence, there is little or almost no variation (in terms of objectives) in the parent population of subsequent generations which hinders the evolution of candidates.

#### 3.5.2. Proposed approach

In order to avoid this problem of premature termination, $\alpha$-DEMO-revised [10] considers propagating only a fraction of $R_{1,G}$. This approach has been extended in DECOR [14] which recommends the elitist selection strategies for different possible proportions of $\left|R_{1,G}\right|$ to $\left|R_{rest,G} = \cup_{q,q\neq 1} R_{q,G}\right|$. The proposed approach of Ensemble of Single Objective Evolutionary Algorithms (ESOEA) adopts this elitist selection strategy which is described as follows:

1. It starts with standard non-dominated sorting using the systematic book-keeping from Ref. [11] with a complexity of $\mathcal{O}\left(M \cdot NP^2\right)$, to obtain $R_{1,G}$ and $R_{rest,G}$ by Eq. (11).
2. Then, based on a parameter $\beta$ which regulates the number of candidates of $\left|R_{1,G}\right|$ and $\left|R_{rest,G}\right|$ allowed to propagate, one of the following approaches (as demonstrated in Fig. 4) is followed:
   - *When* $\left|R_{1,G}\right| > round\,(\beta\% \text{ of } NP)$ *and* $\left|R_{rest,G}\right| > (NP - round\,(\beta\% \text{ of } NP))$:
     For this case, sorting is performed based on secondary selection criteria and from $R_{1,G}$ up to $round\,(\beta\% \text{ of } NP)$ number of candidates are allowed to propagate to $X_{G+1}$.
     The remaining of $X_{G+1}$ is filled set-wise, in the usual way, starting from $R_{2,G}$, each of which can fully be accommodated in $X_{G+1}$

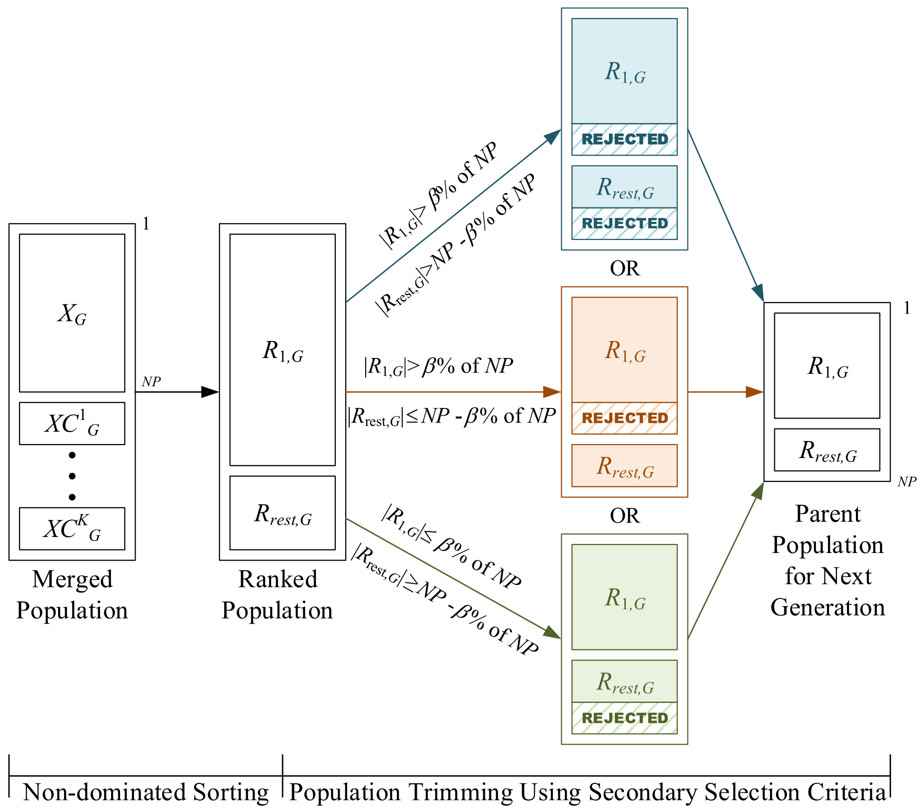


**Fig. 4.** Regulated elitism strategy adopted in this work.

until the last required set $R_{q,G}$ is reached from which only may be a fraction can be accommodated. The elimination of undesired candidates from $R_{q,G}$ is again governed by the secondary selection criteria.

- *When* $|R_{1,G}| > round\,(\beta\%\text{ of }NP)$ *and* $|R_{rest,G}| > (NP - round\,(\beta\%\text{ of }NP))$:
  For this case, the entire of $R_{rest,G}$ is propagated to $X_{G+1}$. From $R_{1,G}$, $\left(NP - |R_{rest,G}|\right)$ number of candidates are allowed to be propagated. Hence, again the elimination of unwanted candidates from $R_{1,G}$ is governed by the secondary selection criteria.
- *When* $|R_{1,G}| \leq round\,(\beta\%\text{ of }NP)$ *and* $|R_{rest,G}| > (NP - round\,(\beta\%\text{ of }NP))$:
  For this case, the usual approach [11] of elitist selection is followed i.e. $X_{G+1}$ is filled set-wise, starting from $R_{1,G}$, each of which can fully be accommodated in $X_{G+1}$ until the last required set $R_{q,G}$ is reached from which only may be a fraction can be accommodated. The elimination of unwanted candidates from $R_{q,G}$ is governed by the secondary selection criteria.
- *When* $|R_{1,G}| < round\,(\beta\%\text{ of }NP)$ *and* $|R_{rest,G}| > (NP - round\,(\beta\%\text{ of }NP))$:
  This case is not possible as $|R_{1,G}| + |R_{rest,G}| \geq NP$.

3. For pruning candidates from a rank of solutions ($R_{q,G}$) in order to obtain a set of solutions of a given size, Algorithm 2 is used to sort the candidates of $R_{q,G}$ from which the required number of candidates are selected, sequentially. In the proposed approach, at first, $d2$ is evaluated for various candidates of $R_{q,G}$ (line 5). Following this, the outer while loop (line 5) determines the various unique directions with which candidates of $R_{q,G}$ are associated. It should be noted that candidate association is not repeated, here. Instead, a vector, called *labels*, is used which passes the indices of the subpopulation/direction with which each candidate of $R_{q,G}$ is associated, either through population partitioning (Section 3.3) or being generated as an offspring from a particular instance of SOEA. Following this, for each unique direction, the candidate from the respective subpopulation within $R_{q,G}$ ($X_{dir}$) with minimum $d2$ is selected ($X_{select}$) and appended at the end of the sorted list of candidates ($X_{sort}$) in line 6–11. Then, $X_{select}$ is removed from $R_{q,G}$ (line 12) and the loop continues until a candidate is chosen from every unique direction. The outer while loop resumes with the reduced set of candidates, $R_{q,G}$ and continues until all candidates of $R_{q,G}$ have been assigned to $X_{sort}$.

Thus, after elitist selection from the merged parent population and child sub-populations of a generation i.e. from $\left(X_G \cup \left(\cup_{k=1}^{K} XC_G^k\right)\right)$, the parent population for the next generation ($X_{G+1}$) is tailored.

### 3.6. Determining sub-population sizes for next generation

This step is performed to impart an adaptive quality to the search for the Pareto-optimal solutions by regulating resource allocation instead of perturbing the uniformly distributed weight vectors. This is the feedback (as shown in Fig. 1) provided to the population decomposition step in terms of sub-population sizes for next generation i.e. $|X_{G+1}^k|$, which assists in re-association of the candidates to the weight vectors. This resource allocation has the following key features:

- The central idea is to allocate more candidates to the poorly performing instances of the single objective evolutionary algorithm (SOEA) (or equivalently to the directions where convergence has difficulty).

**Algorithm 2** Sorting based on Secondary Selection Criteria.
**Input:** $R_{q,G}$: Candidates forming $q$th rank; $F^s(R_{q,G})$: Scaled fitness of $R_{q,G}$; $labels(R_{q,G})$: Subpopulation index with which candidates of $R_{q,G}$ are associated
**Output:** $X_{sort}$: Candidates of $R_{q,G}$ in sorted order; $F^s(X_{sort})$: Scaled fitness of $X_{sort}$

1: **procedure** SECONDSORT($R_{q,G}$, $F^s(R_{q,G})$, $labels(R_{q,G})$)
2: $d2_q = \{d2(X|W_k)|X \in R_{q,G}, k = labels(X)\}$ using Eq. (3) with $F^s(R_{q,G})$
3: $n_{cand} = 1, X_{sort} = \emptyset$
4: **while** $n_{cand} \le \left|R_{q,G}\right|$ **do**
5: $W_{uniq}$ = Obtain unique directions from $labels(R_{q,G})$
6: **for** $dir \in W_{uniq}$ (for each direction) **do**
7: $X_{dir} = \{X \mid X \in R_{q,G}, labels(X) = dir\}$
8: $d2_{dir} = \{d2_i \mid d2_i \in d2_q, labels(X) = dir\}$ with $d2_q$ from line 2
9: $X_{select} = \arg\min_{X \in X_{dir}} d2_{dir}$
10: $X_{sort} = X_{sort} \cup X_{select}$ (append sequentially)
11: $n_{cand} = n_{cand} + 1$
12: $R_{q,G} = R_{q,G} \setminus X_{select}$
13: **end for**
14: **end while**
15: Return $X_{sort}$ and $F^s(X_{sort})$
16: **end procedure**

**Algorithm 3** Generation $G$ of ESOEA/DE procedure.
**Input:** $\{W_k\}$: Set of arrays to define the weight vectors; $X_G$: Parent population; $F(.)$: Fitness function; $\{|X^k|\}$: Set of sub-population sizes; $K$: Number of direction vectors;
**Output:** $X_{G+1}$: Parent population for next generation; $\{|X^k_{G+1}|\}$: Set of sub-population sizes for next generation

1: **procedure** ESOEA/DE($\{W_k\}$, $X_G$, $F(.)$, $\{|X^k_G|\}$, $K$)
2: Get $F^r_G$ using Eq. (6) from $F(X_G)$
3: Get $F^s(X_G)$ with $F^r_G$ and Eq. (7) on all candidates
4: Get $\{X^k_G\}$ = CANDASSOC($\{\overrightarrow{OW_k}\}$, $F^s(X_G)$, $\{|X^k_G|\}$, $K$), $\forall k = 1, 2, \ldots, K$
5: **for** $k = 1$ to $K$ (for each sub-population) **do**
6: Assign $XP^k_{g=1} = X^k_G$
7: **for** $g = 1$ to $G^{inner}_{max}$ (for each SaNSDE-$k$) **do**
8: Get $XC^k_g$ by applying SaNSDE on $XP^k_g$
9: Get $F(XC^k_g)$ and then get $F^s(XC^k_g)$ with $F^r_G$ (from line 2) and using Eq. (7)
10: Get $F_W(XC^k_g)$ by using Eq. (10) with $F^s(XC^k_g)$ and $W_k$
11: Form $XP^k_{g+1}$ by fitness ($F_W(.)$) based selection of candidates from $XC^k_g$ and $XP^k_g$
12: Assign $XP^k_g = XP^k_{g+1}$
13: **end for**
14: Assign $XC^k_G = XP^k_g$
15: **end for**
16: $(R_{1,G}, R_{2,G}, \cdots) = ndsort\left(X_G \cup \left(\cup_{k=1}^K XC^k_G\right)\right)$ with $ndsort(.)$ performing non-dominated sorting as explained in Section 3.5
17: Get parent population for next generation ($X_{G+1}$) using one of the three approaches of selection explained in Section 3.5.2
18: Get $\{|X^k_{G+1}|\}$ by Eq. (13) (adaptive feedback)
19: Return $X_{G+1}$ and $\{|X^k_{G+1}|\}$
20: **end procedure**

- As an indicator of performance, $share^k$ represents the percentage of candidates contributed by the $k$th instance of SOEA (SOEA-$k$) towards the parent population for the next generation as mentioned in Eq. (13) where $NP^k_{child}$ is the number of candidates contributed by the $k$th child sub-population and $NP^{total}_{child}$ is the total number of candidates contributed by all the child sub-populations.
- The size of the $k$th sub-population for the next generation is, then, negatively correlated to the performance indicator of the $k$th instance of SOEA i.e. $share^k$, by the relation proposed in Eq. (13). It is to be noted that Eq. (13) is followed for $G > 1$ and Eq. (8) is followed for $G = 1$ as mentioned in Section 3.3.

$$\left|X^k_{G+1}\right| = \begin{cases} round\left(\left(\dfrac{100 - share^k}{K-1}\right) \times \left(\dfrac{NP}{100}\right)\right), & \text{if } k \neq K \\ NP - \displaystyle\sum_{k=1}^{K-1} \left|X^k_{G+1}\right|, & \text{if } k = K \end{cases} \tag{13}$$

where, $share^k = (NP^k_{child}/NP^{total}_{child}) \times 100$ with

$$NP^k_{child} = \left|XC^k_G \cap X_{G+1}\right| \text{ and } NP^{total}_{child} = \sum_{k=1}^{K} NP^k_{child}$$

Let the example in Table 1 be considered. As can be seen, reference direction 2 does not contribute anything to the parent population of the next generation, whereas, reference direction 3 contributes half of the candidates to the parent population of the next generation. Thus, more

**Table 1**
Example to illustrate adaptive feedback of subpopulation sizes.

| $k$th subpopulation | Contribution of $k$th subpopulation, $NP^k_{child}$ | Performance indicator of $k$th subpopulation, $share^k$ | Subpopulation size before rounding, $\lvert X^k_{G+1}\rvert$ | Subpopulation size after rounding, $\lvert X^k_{G+1}\rvert$ |
|---|---|---|---|---|
| 1 | 10 | 20% | 10.00 | 10 |
| 2 | 0 | 0% | 12.50 | 13 |
| 3 | 25 | 50% | 6.25 | 6 |
| 4 | 10 | 20% | 10.00 | 10 |
| 5 | 5 | 10% | 11.25 | 11 |
| **Total** | **50** | **100%** | **50** | **50** |

resource could be spent to explore the region around reference direction 2 than reference direction 3. The proposed approach tries to provide this feedback in terms of subpopulation size for the next generation. Thus, by the above method, the resource allocation to the $k$th direction ($\overrightarrow{OW_k}$) is boosted (or damped) if it has a lesser (or higher) contribution in forming the parent population of the next generation as compared to other directions.

Adaptively fixing the number of candidates to be associated is a better strategy than exhaustive association (candidate association to nearest direction vector) as illustrated in Fig. 2a and b. The following arguments compare the usual approach with the proposed approach:

- In the concerned example, it can be seen from Fig. 2a that by following exhaustive association (such as in NSGA-III [38]), $X_1$ will be associated with the direction vector $\overrightarrow{OW_1}$ whereas $X_2$ and $X_3$ will be associated with the direction vector $\overrightarrow{OW_2}$.
- Let the neighborhood around the direction vector $\overrightarrow{OW_1}$ be a more difficult region for optimization (having less density of feasible points) than the neighborhood around the direction vector $\overrightarrow{OW_2}$. This is supported by the fact that more objective vectors have appeared around $\overrightarrow{OW_2}$ than around $\overrightarrow{OW_1}$.
- In the concerned example, let $X_1$ be generated by SOEA-1, and $X_2$ and $X_3$ be generated by SOEA-2, by following the proposed framework. Thus, by Eq. (13), for the next generation, the population for SOEA-1 should have 2 candidates whereas the population for SOEA-2 should have 1 candidate. Using the proposed randomized candidate association (Algorithm 1), it can be seen from Fig. 2a that with $W_2$ being the randomly chosen reference direction $W_r$ and $\phi_{3r} < \phi_{2r} < \phi_{1r}$, $X_3$ will be associated with $\overrightarrow{OW_2}$ whereas $X_1$ and $X_2$ will be associated with $\overrightarrow{OW_1}$. The same allocation occurs even if $W_1$ is the randomly chosen reference direction $W_r$.
- This randomized association makes more sense in this case, as the neighborhood of $\overrightarrow{OW_1}$ is less explored. Thus, allocating more number of candidates for SOEA-1 increases the possibility of exploitation of the unexplored region and thereby, assisting in improving the overall diversity of the Pareto-optimal set.

An interesting observation is that although the sub-population for the least contributing SOEA (with minimum $share^k$) gets the highest number of candidates from the parent population, yet the proposed candidate association approach does not choose the direction corresponding to least contributing SOEA as the reference direction $W_r$, rather a random direction is chosen (line 2 of Algorithm 1). This step ensures that the proposed candidate association is not greedy.

### 3.7. Discussion

The term $d1$ and $d2$ of the PBI strategy is demonstrated in Fig. 5a. Assuming the objective vectors have been translated in the first hyper-octant, the term $d1$ used in PBI function of Eq. (10) involves the factor shown in Eq. (14) i.e. the projection of the objective vector on the weight vector.

$$\overrightarrow{OF(X_i^k)} \cdot \overrightarrow{OW_k} = \left\|\overrightarrow{OF(X_i^k)}\right\| \cdot \left\|\overrightarrow{OW_k}\right\| \cdot \cos(\phi_{ik}) \tag{14}$$

Given that $d1$ is later normalized by the magnitude of the weight vector $\left\|\overrightarrow{OW_k}\right\|$ for all the candidates of the $k$th sub-population as shown in Eq. (3), for minimization of $F_W(.)$ the following scenarios occur:

- Minimization of $\left\|\overrightarrow{OF(X_i^k)}\right\|$ implies an improvement in convergence. This is demonstrated by Fig. 5a where $\phi_{1k} = \phi_{2k} = \phi_{3k} = \phi$ and $\left\|\overrightarrow{OF(X_1^k)}\right\| > \left\|\overrightarrow{OF(X_2^k)}\right\| > \left\|\overrightarrow{OF(X_3^k)}\right\|$ indicate the projections of three objective vectors on the weight vector is gradually decreasing from candidate 1 to 3 i.e. $d1(X_1^k) > d1(X_2^k) > d1(X_3^k)$.
- Another parameter, that can affect the minimization of $d1(X_i^k)$, is $\phi_{ik}$. Minimization of $d1(X_i^k)$ requires maximization of $\phi_{ik}$ from 0 to

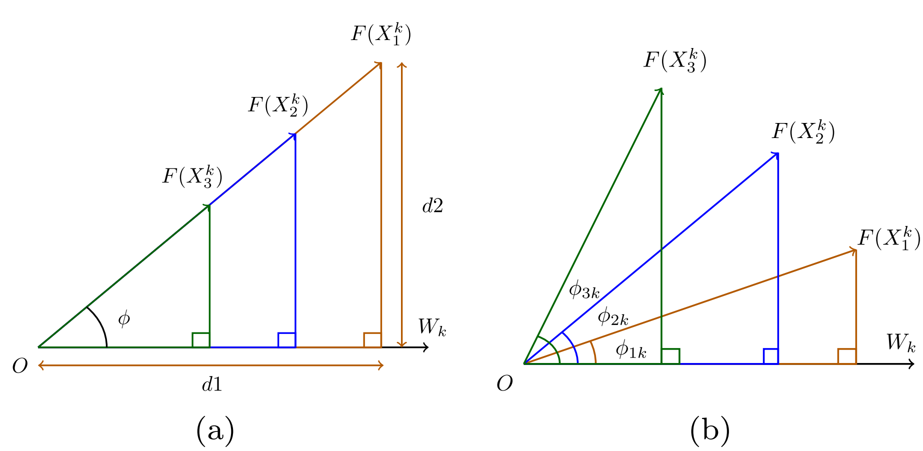


**Fig. 5.** Interpretation of transforming objective space for optimization: (a) when only magnitude of objective vectors is changing, (b) when only angle between objective vectors and the reference weight vector is changing.

$(\pi/2)$ radians, but this disturbs the diversity established during population decomposition. The disrupted diversity is re-established by repeating candidate association adaptively after periodic intervals of generations. However, as reproduction operators tend to generate child candidates in the neighborhood of the parent candidates [15,46], chances are less that a child candidate moves very far away (in terms of $\phi_{ik}$) from parent candidates within a small number of generations ($G_{max}^{inner}$) in order to disrupt the established diversity. This case is demonstrated in Fig. 5b where $\phi_{1k} < \phi_{2k} < \phi_{3k}$ and $\left\|\overrightarrow{OF(X_1^k)}\right\| = \left\|\overrightarrow{OF(X_2^k)}\right\| = \left\|\overrightarrow{OF(X_3^k)}\right\|$ indicate the projections of three function vectors on the weight vector is gradually decreasing from candidate 1 to 3 (indicating minimization) i.e. $d1(X_1^k) > d1(X_2^k) > d1(X_3^k)$.

- Thus, although $d1$ can assist in improving the convergence, it can disrupt the diversity to some extent. To combat this problem, the term $d2$ assists which is essentially the magnitude of the vector difference between the objective vector and its projection of objective vector along the weight vector. As shown in Fig. 5a, with a decrease in the magnitude of the objective vector from candidate 1 to candidate 3, $d2$ also decreases i.e. $d2(X_1^k) > d2(X_2^k) > d2(X_3^k)$. On the other hand, with a constant magnitude of the objective vector, as the candidate moves closer to the weight vector, its $d1$ increases but $d2$ decreases as seen in Fig. 5b from candidate 3 to 1 i.e. $d2(X_3^k) > d2(X_2^k) > d2(X_1^k)$. Hence, to balance between convergence and diversity, the penalty parameter $\theta$ is used in Eq. (3).
- Due to difficult search regions in the objective space, a special case may arise, where a candidate gets associated with a particular direction in every alternate population decomposition stages, without much change in the magnitude of the objective vector. However, the effort to propagate some candidates from each subpopulation to the next generation (Algorithm 2), tends to discover some solutions eventually along all directions for MaOO problems with regular Pareto-fronts even with difficult search regions. Nonetheless, if the convergence does not improve at all for such a candidate as expected for problems with disconnected Pareto-front, it will have much lesser survival chances during the intermediate elitist selection stages as it will eventually be dominated by other candidates (associated with other directions). This ensures convergence for the different types of MaOO problem using the proposed framework (Eq. (10)).

Thus, in general, optimization of $F_W(.)$ primarily targets at improving convergence of the non-dominated set of solutions along the $K$ directions in the objective space, considering the diversity characteristic has already been embedded during the population decomposition stage.

The similarities and differences in the proposed framework of ESOEA with a few related works viz. MOEA/D-M2M [36], MOEA/DD [15], RVEA [48], AR-MOEA [47] are highlighted next.

#### 3.7.1. *Similarities with related algorithms*

The following similarities are observed between ESOEA and other related algorithms:

a) Similar to MOEA/D-M2M and RVEA, ESOEA uses acute angle (Eq. (9)) between objective vectors and reference vectors for association of candidates.
b) Similar to MOEA/DD, ESOEA uses PBI as the scalarization function.
c) Similar to MOEA/D-M2M, MOEA/DD and AR-MOEA, ESOEA employs Pareto-dominance relation to partition the set of discovered candidates into non-dominated ranks of solutions. Although RVEA does not use Pareto-dominance during selection, similar to it, ESOEA also performs an elitist selection from the merged parent and offspring populations.
d) Similar to MOEA/DD and MOEA/D-M2M, ESOEA exploits the neighborhood property of MaOO problems during mating of candidates.

#### 3.7.2. *Differences with related algorithms*

The following differences are observed between ESOEA and other related algorithms:

a) *With MOEA/D-M2M:* During the selection step of MOEA/D-M2M [36], an exhaustive association of candidates to reference direction occurs, followed by the selection of candidates while maintaining a predetermined subpopulation size. If a sub-population size exceeds this predetermined size, the usual non-dominated sorting based selection [11,36] is performed, otherwise, candidates are randomly selected from the rest of the population to fill up the respective subpopulation. Unlike this, ESOEA uses randomized association, adaptive subpopulation size, regulated scheme of non-dominated sorting and preserves the neighborhood property during formation of parent subpopulations.
b) *With MOEA/DD:* In MOEA/DD [15], mating occurs either between solutions from neighboring subpopulation or randomly from the global population, whereas in ESOEA, mating occurs only within each subpopulation. Moreover, MOEA/DD uses steady-state selection scheme where isolated solution even with worst scalarized fitness in the last domination level survives an extra iteration. ESOEA intends to achieve a similar goal by propagating the best solution, associated with each reference direction, within a non-dominated rank of solutions.
c) *With RVEA:* In RVEA [48], mating occurs between candidates chosen randomly from the global population. Also, during the selection step of RVEA [48], an exhaustive association of candidates occurs, followed by APD-guided selection. Moreover, RVEA uses reference vector adaptation for scaled MaOO problems and reference vector regeneration for irregular Pareto-fronts. Unlike this, ESOEA performs mating within each subpopulation, uses randomized association, performs selection guided by Pareto-dominance and PBI, and keeps the initial distribution of reference vectors unperturbed.
d) *With AR-MOEA:* In the selection step of AR-MOEA [47], the entire rank-one solution is propagated to the next generation, followed by secondary selection depending on the selection of least contributing solutions from the last essential front using IGD-NS. Also, AR-MOEA will require new reproduction operators for handling problems where parts of Pareto-fronts cannot be easily obtained [47]. Unlike this, ESOEA performs regulated selection based on Pareto-dominance and PBI, and is capable of guiding the search process towards reference directions where it is difficult to discover solutions.

This adaptive framework of Ensemble of Single Objective Evolutionary Algorithms (ESOEA) is implemented to assess its efficacy whose details are mentioned in the following Section.

## 4. Performance analysis

The proposed work is implemented Matlab R2017a using a 64-bit computer with 8 GB RAM and Intel Core i7 @2.20 GHz processor. The experimental specifications in terms of benchmark test problems, performance indicators and parameter setting for performance analysis the proposed framework (Fig. 1), are discussed in detail subsequently. Following this, the efficacy of ESOEA is assessed by comparing its performance with several other state-of-the-art approaches noted over 30 independent runs of the algorithms. Results of some miscellaneous experiments are also provided to establish the importance of a few modules of the proposed framework.

### 4.1. *Benchmark problems*

For testing the efficacy of several kinds of box-constrained $M$-objective optimization algorithms, there is a handful of benchmark problems in literature. Among these, DTLZ test suite [10,38,56] and WFG test suite [10,38,57] are the most widely studied ones. Recently, for investing the performance of $M$-objective algorithms, the IMB test suite containing problems with imbalance mapping and variable linkage difficulties has also been proposed in Ref. [37]. Additionally, for comparison of ESOEA/DE with ensemble methods in multi-objective evolutionary algorithms, test instances from CEC 2009 competition have been considered.

From the DTLZ [3,14,56,58] test suite, DTLZ1, DTLZ2, DTLZ3, DTLZ4 and DTLZ7 are chosen. DTLZ2 and DTLZ4 are unimodal problems, whereas DTLZ1 and DTLZ3 are multi-modal problems. DTLZ7, on the other hand, is interesting due to the disconnected nature of its Pareto-front. As per the specifications in Refs. [10,56,58], the number of decision variables, for an $M$-objective DTLZ problem, is $N = M + s - 1$ where $s = 5$ for DTLZ1, $s = 20$ of DTLZ7 and $s = 10$ for DTLZ2, DTLZ3 and DTLZ4 problems.

From the WFG [10,38,57] test suite, WFG1 and WFG2 are chosen for assessment of the proposed work as these problems have Pareto-fronts with sharp tails and disconnected Pareto-fronts, respectively. For $M$-objective WFG1 and WFG2 problems, the number of decision variables is set as $N = 24$ with $(M-1)$ position-related variables and $(N-M+1)$ distance-related variables. Only for WFG2 problems with even number of objectives, $N$ is set to 23 as it requires an even number of distance related variables due to its nature of non-separable reductions [57].

From the IMB test suite [37], IMB1 to IMB10 problems are studied. This test suite is challenging as it is characterized by regions in search space, which are difficult to be explored. Out of these, IMB1 to IMB6 problems exhibit imbalance mapping difficulty whereas IMB7 to IMB10 problems exhibit variable linkage difficulty. As per the recommendation in Ref. [37], $N = 10$ is chosen for all IMB problems.

From the set of box-constrained problems of CEC 2009 competition [59], UF1 to UF10 are considered for performance analysis of ESOEA/DE. This test suite stimulates the research on multi-objective evolutionary algorithms by presenting test cases bearing resemblance with complicated real-life problems. As per the recommendation in Ref. [59], $N = 30$ is chosen for all CEC 2009 test instances.

### 4.2. Performance indicators

The solution from an $M$-objective optimization algorithm is the Pareto-optimal solution ($PS$) and Pareto-front ($PF$). In this work, the quality of the obtained solution is assessed in terms of convergence metric [3,10,60], inverted generational distance (IGD) [1,2,5] and hypervolume indicator [10,14,27]. Moreover, the proposed work visualizes some $PF$ using 2 or 3-dimensional Cartesian coordinate plots for problems with 2 or 3 objective problems, respectively, and using spherical coordinate plots [61] for other problems.

Evaluation of convergence metric and IGD metric are very similar. However, the former solely represents convergence, whereas the latter represents both convergence and diversity of the $PF$. These indicators are recorded for the DTLZ and WFG problems. A reference set ($H$) is required to represent the true $PF$. For DTLZ1 to DTLZ4, $H$ is constructed in a similar fashion as done in Refs. [15,47] i.e. $H$ is formed by the points on the true $PF$ where the reference vectors defined by Das and Dennis's approach intersect. For these problems, $|H|$ is approximately considered to be 5000 as in Ref. [47]. For DTLZ7, WFG1, WFG2, and for CEC 2009 test instances (except UF5[1]), several points on the true $PF$ are randomly sampled to yield $H$ such that $|H| = 5000$ as in Refs. [10,14]. Convergence metric ($\delta_{PF}$) is estimated by Eq. (15) as the sample mean of the minimum Euclidean distance $D(.)$ of the candidates in $PF$ from $H$, over the number of solutions in the obtained $PF$. On the other hand, IGD metric ($I_{PF}$) is estimated by Eq. (16) as the sample mean of the minimum Euclidean distance $D(.)$ of the candidates in $H$ from $PF$, over the number of solutions in the obtained $H$. Thus, lower values of $\delta_{PF}$ and $I_{PF}$ indicate better $PF$.

$$\delta_{PF} = \frac{1}{|PF|}\sum_{i=1}^{|PF|}\left(\min_{j=1}^{|H|} D\left(F\left(Y_i\right), H_j\right)\right), \quad \forall F(Y_i) \in PF \text{ and } H_j \in H \tag{15}$$

$$I_{PF} = \frac{1}{|H|}\sum_{j=1}^{|H|}\left(\min_{i=1}^{|PF|} D\left(F\left(Y_i\right), H_j\right)\right), \quad \forall F(Y_i) \in PF \text{ and } H_j \in H \tag{16}$$

Hypervolume indicator ($\mathcal{H}_{PF}$) measures the convergence as well as the diversity of the obtained $PF$ [10,27]. It is estimated as the ratio of volume Pareto-dominated by the obtained $PF$ to the total volume of a hyper-rectangle defined with respect to the origin and a reference point ($F_{ref}$) in the objective space as shown in Eq. (17). For estimating $\mathcal{H}_{PF}$, a set of points ($H$) is sampled by Monte-Carlo simulations [10,27] inside the hyper-rectangle, out of which the subset of $H$ that is Pareto-dominated by $PF$ (Eq. (2)) is obtained using the binary-valued attainment function ($\alpha\left(H_j, PF\right)$) for all constituents ($H_j$) of $H$ with respect to the constituents ($F\left(Y_i\right)$) of $PF$. The values of $|H|$ and $F_{ref}$ are specified later corresponding to each experiment where results are noted.

$$\mathcal{H}_{PF} = \frac{1}{|H|}\sum_{j=1}^{|H|}\alpha\left(H_j, PF\right) \text{ where, } H_j \in H \text{ and } \quad \alpha\left(H_j, PF\right) = \begin{cases} 1, & \text{if } \exists F(Y_i) \in PF \text{ with } F(Y_i) \prec H_j \\ 0, & \text{otherwise} \end{cases} \tag{17}$$

### 4.3. Experimental settings of ESOEA

For implementing the proposed framework, Differential Evolution with Self-adaptive Neighborhood Search (SaNSDE) [62] is used as the base optimizer of the ensemble of SOEA. The parameters of SaNSDE are learned adaptively and, in turn, could address subregion-specific characteristics of the fitness landscape. The parameters [62] viz. scale factor (sampled from normal or Cauchy distribution), mutation probability (to choose between DE/rand/1/bin and DE/current-to-best/2/bin) and crossover rate (sampled from normal distribution) are learned over every subpopulation and updated after every generation until $G_{max}^{inner}$. For every generation of the central loop, the learning of parameters of SaNSDE is repeated. The central loop is terminated after $G_{max}^{outer}$ which yields the final $PF$. This entire framework is referred to as ESOEA/DE, hereafter, and its steps are summarized in Algorithm 2 for a single generation of the central loop.

The values of $G_{max}^{inner}$ and $G_{max}^{outer}$ have been tuned for the considered test problems and are mentioned in Table 2. Also, the divisions of the two layers (Eq. (4)) considered for distributing weight vectors ($\{W_k\}$) are mentioned in Table 2. As $M$ increases, multi-modal problems (DTLZ1 and DTLZ3) and problems with sharp-tailed $PF$ (WFG1) are observed to require higher $G_{max}^{inner}$ (indicating irregular landscape) whereas unimodal problems (DTLZ2 and DTLZ4) needed higher $G_{max}^{outer}$ (indicating smoother and flat regions in landscape). While all IMB1-10 and UF1-10 are 2- or 3-objective problems, IMB problems require lesser generations to converge. This may be attributed to the requirement of a lesser number of decision variables ($N$) for defining the IMB test problems. Among the remaining parameters for ESOEA/DE, the subproblem sizes are initialized to 10 which is later adaptively adjusted by Eq. (13). Thus, the global population size is 10 times the number of weight vectors for each test problem. The penalty parameter ($\theta = 5$) for PBI is set as per the specifications in Refs. [15,18] and the parameter ($\beta = 0.75$) for the proposed elitist selection approach (Section 3.5.2) is set as per the specifications in Refs. [3,10,14].

[1] Pareto-front of UF5 consists of $(2s + 1)$ discrete Pareto-optimal solutions with $s = 10$ [59].

**Table 2**
Values of $G_{max}^{inner}$ (tuned in the range 10–30) and $G_{max}^{outer}$ (tuned in the range 25–350) for various different test problems, and the number of divisions for boundary layer ($p_1$) and inside layer ($p_2$) for defining the weight vectors for different number of objectives.

| Problems | $M = 3$ | $M = 5$ | $M = 10$ | $M = 20$ | Problems | $M = 2$ | $M = 3$ | Problems | $M = 2$ | $M = 3$ |
|---|---|---|---|---|---|---|---|---|---|---|
| DTLZ1 | 20 and 35 | 10 and 150 | 30 and 50 | 30 and 70 | IMB1 | 10 and 20 | – | UF1 | 20 and 50 | – |
| DTLZ2 | 10 and 25 | 10 and 50 | 10 and 200 | 10 and 250 | IMB2 | 10 and 100 | – | UF2 | 20 and 50 | – |
| DTLZ3 | 10 and 100 | 20 and 50 | 20 and 75 | 20 and 100 | IMB3 | 20 and 50 | – | UF3 | 30 and 250 | – |
| DTLZ4 | 10 and 50 | 10 and 100 | 10 and 200 | 10 and 350 | IMB4 | – | 10 and 50 | UF4 | 20 and 75 | – |
| DTLZ7 | 20 and 25 | 20 and 50 | 20 and 100 | 20 and 100 | IMB5 | – | 10 and 20 | UF5 | 30 and 300 | – |
| WFG1 | 30 and 50 | 10 and 200 | 20 and 100 | 20 and 125 | IMB6 | – | 10 and 20 | UF6 | 20 and 150 | – |
| WFG2 | 10 and 50 | 10 and 75 | 30 and 50 | 10 and 150 | IMB7 | 10 and 75 | – | UF7 | 20 and 100 | – |
| | | | | | IMB8 | 10 and 80 | – | UF8 | – | 30 and 300 |
| | | | | | IMB9 | 10 and 100 | – | UF9 | – | 30 and 50 |
| | | | | | IMB10 | – | 20 and 50 | UF10 | – | 30 and 150 |
| $p_1, p_2$ | 13, 0 | 6, 0 | 3, 2 | 2, 1 | $p_1, p_2$ | 100, 0 | 13, 0 | $p_1, p_2$ | 100, 0 | 13, 0 |

**Table 3**
IGD values of NSGA-II, MOEA/D, AR-MOEA and ESOEA/DE from 30 independent runs for 3-objective problems with regular and irregular Pareto-fronts.

| Problems | $M$ | NSGA-II | MOEA/D | AR-MOEA | ESOEA/DE |
|---|---|---|---|---|---|
| DTLZ1 | 3 | 2.6772E-02 ± 1.36E-03(+) | 1.8973E-02 ± 3.89E-05(+) | 1.8972E-02 ± 3.52E-05(+) | **1.1561E-02 ± 1.75E-03** |
| DTLZ2 | 3 | 6.7599E-02 ± 2.65E-03(+) | 5.1303E-02 ± 4.38E-04(+) | 5.0244E-02 ± 6.34E-05(+) | **4.6183E-02 ± 1.75E-03** |
| DTLZ3 | 3 | 1.0247E-01 ± 1.73E-01(+) | 5.4281E-02 ± 2.52E-03(≈) | **5.2839E-02 ± 1.67E-03**(−) | 5.4789E-02 ± 8.58E-04 |
| DTLZ4 | 3 | 1.2481E-01 ± 2.23E-01(+) | 4.1204E-01 ± 3.65E-01(+) | 1.6466E-01 ± 2.11E-01(+) | **5.6493E-02 ± 8.46E-04** |
| DTLZ7 | 3 | 7.4897E-02 ± 3.32E-03(+) | 1.2746E-01 ± 1.48E-03(+) | 6.2010E-02 ± 9.20E-04(+) | **3.4653E-02 ± 2.63E-03** |
| WFG1 | 3 | 2.5333E-01 ± 3.02E-02(+) | 3.6315E-01 ± 3.72E-02(+) | **1.5906E-01 ± 1.17E-02**(≈) | 1.6003E-01 ± 9.39E-03 |
| WFG2 | 3 | 1.9063E-01 ± 1.27E-02(+) | 9.5329E-01 ± 7.30E-02(+) | 1.7238E-01 ± 4.52E-03(+) | **1.4627E-01 ± 9.83E-04** |
| +/ − / ≈ | | 7/0/0 | 6/0/1 | 5/1/1 | |

With these settings, ESOEA/DE is executed for 30 independent runs for various test problems and are compared subsequently. In each of the experiments, the best and the second best values are highlighted in the results with dark gray and light gray background, respectively. Moreover, all the results have also been statistically validated using the two-tailed paired $t$-test [10] for all the test cases, under the assumption of the null hypothesis that the performance of ESOEA/DE is equivalent to other competitor algorithms. The $p$-values are noted for a 95% confidence interval and the significance is indicated using three signs viz. + denoting the performance of ESOEA/DE is significantly better (i.e. $p \leq 0.05$, rejecting null hypothesis), − denoting the performance of the competitor algorithm is significantly better than ESOEA/DE (i.e. $p \leq 0.05$, rejecting null hypothesis) and ≈ indicating the performance of ESOEA/DE and the competitor algorithm is equivalent (i.e. $p > 0.05$ not being able to reject the null hypothesis).

### 4.4. Effectiveness of ESOEA/DE to address MOO problems

In this experiment, the IGD values of several 3-objective test problems obtained by ESOEA/DE are noted in Table 3. These values are compared with those obtained by the two most popular MOEAs viz. NSGA-II [11] and MOEA/D [32], and a state-of-the-art approach viz. AR-MOEA [47]. These competitor algorithms are set as per the specifications in Ref. [47]. The results show that ESOEA/DE has outperformed these algorithms in most of the test cases and in cases where ESOEA/DE has failed to outperform the best performing algorithm, the IGD values are not very different.

To support these IGD values, *PF* obtained by ESOEA/DE for the MOO problems are visualized in Fig. 6. The Pareto-fronts of DTLZ2, DTLZ3 and DTLZ4 are identical. For DTLZ7, the disconnected Pareto-optimal patches have been explored. For WFG1, the outline of the *PF* and a part of its sharp tail have been discovered.

Although these experiments establish the efficacy of the ESOEA/DE for addressing MOO problems, MOEA/D-M2M [36,37] has been designed for a special class of difficult MOO problems. Such difficulties are found in the IMB test suite and hence, the performance of ESOEA/DE is studied on the IMB test problems using hypervolume indicator with $|H| = 10000$, $F_{ref} = [1,1]$ (for 2-objective problems) or $F_{ref} = [1,1,1]$ (for 3-objective problems). The hypervolume values are noted in Table 4 and *PF* of IMB problems are shown in Fig. 7. These values compared with MOEA/D [32] and MOEA/D-M2M [37], which are set up using the specifications in Ref. [37]. As noted in Table 4 and Fig. 7d and j, although ESOEA/DE is capable of finding solutions in the difficult regions, it has not shown superior performance for IMB4 and IMB10 problems. Also, for the worst cases (Table 4), M2M approach has better performance than ESOEA/DE. This is because unlike ESOEA

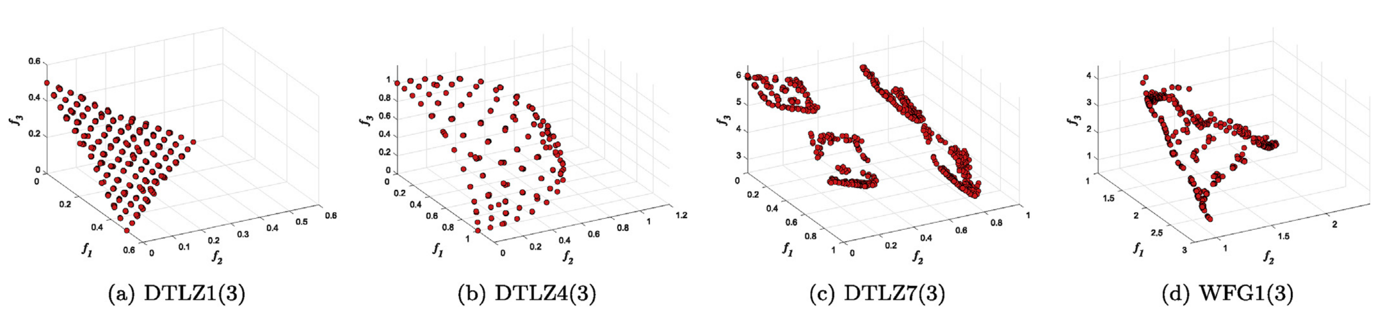

**Fig. 6.** Pareto-fronts obtained through ESOEA/DE for 3-objective test problems.

**Table 4**
Best, mean and worst hypervolume values of MOEA/D, MOEA/D-M2M and ESOEA/DE from 30 independent runs for each IMB problems.

| IMB Test | MOEA/D | | | MOEA/D-M2M | | | ESOEA/DE | | |
|---|---|---|---|---|---|---|---|---|---|
| Problems | best | mean | worst | best | mean | worst | best | mean | worst |
| IMB1 | 0.4684 | 0.4207 | 0.4154 | 0.6387 | 0.6375 | 0.6354 | **0.6712** | **0.6640** | **0.6569** |
| IMB2 | 0.4436 | 0.3840 | 0.3390 | 0.4627 | 0.4608 | 0.4583 | **0.4902** | **0.4838** | **0.4700** |
| IMB3 | 0.0385 | 0.0385 | 0.0385 | 0.1851 | 0.1836 | **0.1824** | **0.1923** | **0.1838** | 0.1728 |
| IMB4 | 0.7361 | 0.7122 | 0.7030 | **0.7803** | **0.7795** | **0.7785** | 0.7716 | 0.7599 | 0.7488 |
| IMB5 | 0.3916 | 0.3913 | 0.3910 | 0.4266 | 0.4229 | 0.4202 | **0.4306** | **0.4247** | **0.4205** |
| IMB6 | 0.7783 | 0.7758 | 0.7751 | 0.7916 | 0.7909 | **0.7904** | **0.7998** | **0.7921** | 0.7843 |
| IMB7 | 0.6327 | 0.6325 | 0.6322 | 0.6545 | 0.6540 | **0.6534** | **0.6682** | **0.6559** | 0.6415 |
| IMB8 | 0.4504 | 0.4500 | 0.4496 | 0.4840 | **0.4830** | **0.4820** | **0.4885** | 0.4770 | 0.4676 |
| IMB9 | 0.1716 | 0.1713 | 0.1712 | 0.1975 | **0.1960** | **0.1946** | **0.1989** | 0.1951 | 0.1911 |
| IMB10 | 0.7815 | 0.7812 | 0.7807 | **0.7849** | **0.7842** | **0.7835** | 0.7698 | 0.7668 | 0.7613 |

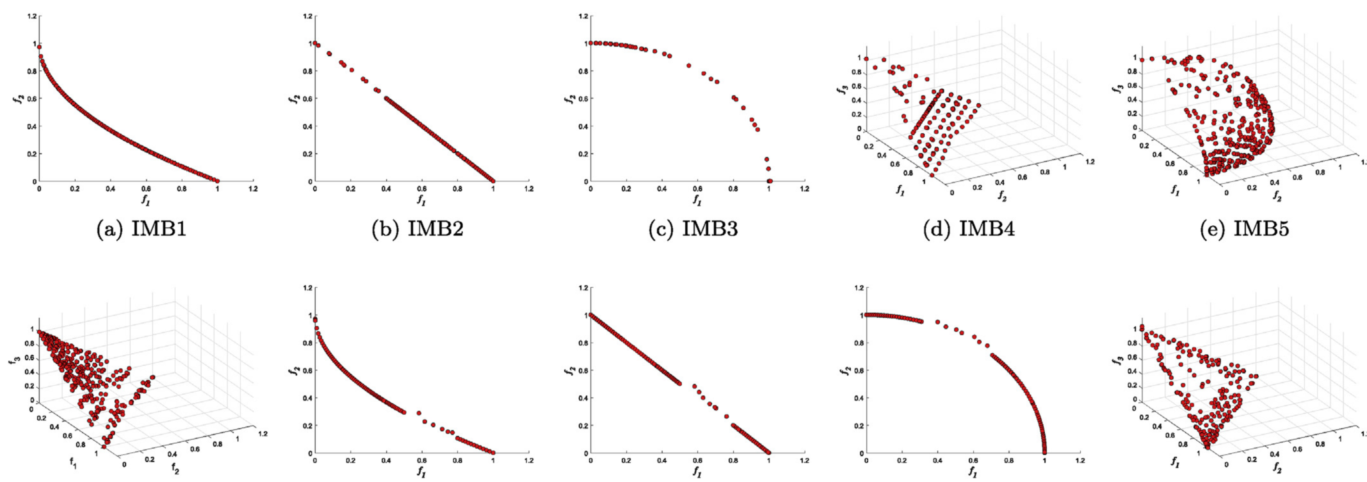

(a) IMB1 (b) IMB2 (c) IMB3 (d) IMB4 (e) IMB5

(f) IMB6 (g) IMB7 (h) IMB8 (i) IMB9 (j) IMB10

**Fig. 7.** Pareto-fronts obtained through ESOEA/DE for IMB test problems.

which decomposes a MOO into multiple single objective problems, M2M approach decomposes a MOO into multiple simpler MOO problems. Thus, a combination of *PF* of simpler MOO problems is equivalent to the *PF* of the original MOO problem, whereas a combination of solutions of single objective problems is only an approximation to the *PF* of the original MOO problem [36]. Nonetheless, for most of the IMB problems, ESOEA/DE performs better than MOEA/D and MOEA/D-M2M on best cases and also on some average cases. The capability of ESOEA/DE in finding solutions even in difficult regions is because of its adaptive feedback strategy and adaptive parameters of base optimizers.

A recent literature survey [63] mentioned various ensemble methods in evolutionary algorithms. It is only fair to compare the proposed approach viz. ESOEA, which is also a population-based optimization using ensemble strategies. However, there are only a few ensemble methods for multi-objective optimization out of which the decomposition based algorithms are MOEA/D-DRA [64] and ENS-MOEA/D [65]. As there is a multitude of reproduction operators with each having their

**Table 5**
IGD values of experiments on ESOEA/DE from 30 independent runs for CEC 2009 competition problems with regular and irregular Pareto-fronts.

| Problems | MOEA/D-DRA | ENS-MOEA/D | ESOEA/DE |
|---|---|---|---|
| UF1 | 4.2920E-03 ± 2.63E-04 (−) | **1.6423E-03 ± 1.26E-04** (−) | 7.3920E-03 ± 2.83E-03 |
| UF2 | 5.6150E-03 ± 4.12E-04 (+) | 4.0487E-03 ± 1.01E-03 (≈) | **3.5153E-03 ± 3.56E-04** |
| UF3 | 1.1165E-02 ± 1.31E-02 (−) | **2.5916E-03 ± 4.56E-04** (−) | 2.9207E-02 ± 1.15E-02 |
| UF4 | 6.4145E-02 ± 4.24E-03 (+) | 4.2070E-02 ± 1.33E-03 (+) | **1.3010E-02 ± 4.89E-04** |
| UF5 | 4.1851E-01 ± 1.36E-01 (+) | 2.4811E-01 ± 4.26E-02 (+) | **7.0236E-02 ± 1.37E-02** |
| UF6 | 3.2736E-01 ± 1.86E-01 (+) | 6.0847E-02 ± 1.98E-02 (+) | **3.8250E-02 ± 3.67E-03** |
| UF7 | 6.2620E-03 ± 3.31E-03 (+) | **1.7286E-03 ± 8.52E-04** (−) | 5.2724E-03 ± 4.50E-04 |
| UF8 | 5.7443E-02 ± 3.37E-03 (+) | 3.1006E-02 ± 3.01E-03 (+) | **2.6375E-02 ± 3.21E-03** |
| UF9 | 9.7693E-02 ± 5.43E-02 (+) | **2.7874E-02 ± 9.57E-03** (−) | 4.0991E-02 ± 6.99E-03 |
| UF10 | 4.6265E-01 ± 3.87E-02 (+) | 2.1173E-01 ± 1.99E-02 (≈) | **1.9602E-01 ± 4.00E-02** |
| +/ − / ≈ | 8/2/0 | 4/4/2 | |

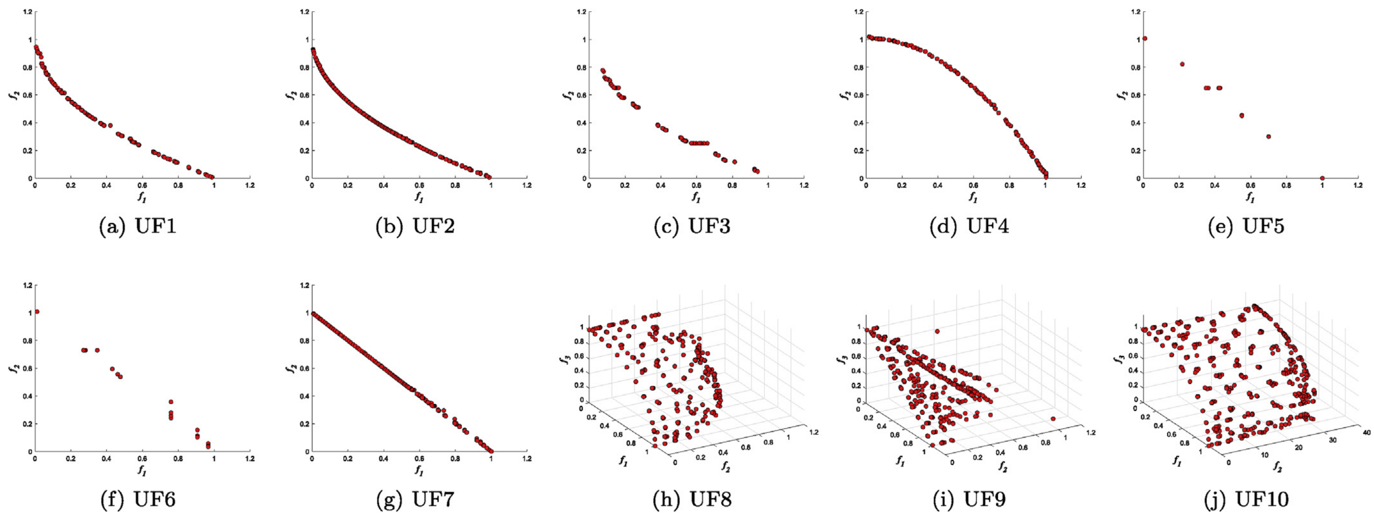


**Fig. 8.** Pareto-fronts obtained through ESOEA/DE for CEC 2009 test instances.

**Table 6**
Convergence metric values of ESOEA/DE and various other kinds of evolutionary algorithms from 30 independent runs for DTLZ problems.

| Problems | $M$ | NSGA-II | MOEA/D | HypE | DEMO | $\alpha$-DEMO-r | ESOEA/DE |
|---|---|---|---|---|---|---|---|
| DTLZ1 | 10 | 225.4502 ± 5.9816(+) | 2.4800 ± 1.0351(+) | 146.3039 ± 2.2147(+) | 142.2519 ± 3.1073(+) | **0.1098 ± 0.0201**(−) | 0.2455 ± 0.0523 |
| | 20 | 176.2357 ± 3.6600(+) | 3.2397 ± 1.1651(+) | 305.1945 ± 9.7488(+) | 143.5408 ± 2.7434(+) | 1.2356 ± 0.0210(+) | **0.3491 ± 0.0405** |
| DTLZ2 | 10 | 1.4716 ± 0.0317(+) | 0.7419 ± 0.0101(+) | 1.3979 ± 0.0156(+) | 1.3891 ± 0.0161(+) | **0.0741 ± 0.0012**(−) | 0.6132 ± 0.0078 |
| | 20 | 1.9273 ± 0.0224(+) | 1.3116 ± 0.0050(+) | 1.9240 ± 0.0144(+) | 1.9009 ± 0.0092(+) | **0.8912 ± 0.0150**(−) | 1.2169 ± 0.0367 |
| DTLZ3 | 10 | 1048.0740 ± 39.3631(+) | 24.8627 ± 4.5587(+) | 409.5137 ± 3.9870(+) | 939.7426 ± 9.8824(+) | 5.7898 ± 0.0922(+) | **0.8351 ± 0.0565** |
| | 20 | 978.3490 ± 44.9975(+) | 37.8409 ± 7.2125(+) | 911.8077 ± 5.5582(+) | 1024.4046 ± 12.5577(+) | 45.5263 ± 0.7134(+) | **1.3600 ± 0.0090** |
| DTLZ4 | 10 | 1.1784 ± 0.0264(+) | 0.7461 ± 0.0102(+) | 0.8914 ± 0.0106(+) | 1.2663 ± 0.0347(+) | **0.5112 ± 0.0089**(−) | 0.6118 ± 0.0088 |
| | 20 | 1.4337 ± 0.0309(+) | 1.0818 ± 0.0070(+) | 0.9572 ± 0.0077(−) | 1.6816 ± 0.0370(+) | **0.7701 ± 0.0127**(−) | 0.9771 ± 0.0076 |
| DTLZ7 | 10 | 42.6764 ± 0.7278(+) | 2.3922 ± 0.1161(+) | 40.0715 ± 0.2762(+) | 41.6292 ± 0.2632(+) | 5.8112 ± 0.0972(+) | **0.5856 ± 0.0090** |
| | 20 | 78.0439 ± 0.4853(+) | 6.8244 ± 0.5152(+) | 82.4481 ± 0.3383(+) | 84.4237 ± 0.5181(+) | 5.6797 ± 0.0989(+) | **1.7615 ± 0.1327** |
| +/ − / ≈ | | 10/0/0 | 10/0/0 | 9/1/0 | 10/0/0 | 5/5/0 | |

own benefits, the work in MOEA/D-DRA proposes adaptive switching between simplex and center of mass crossover operators [64]. As neighborhood size plays a vital role in MOEA/D, in order to make this parameter adaptive, an ensemble of neighborhood sizes is used in ENS-MOEA/D [65]. The values for IGD metric when ESOEA/DE is applied to UF1 to UF10 are noted in Table 5 along with the IGD values for applying ENS-MOEA/D and MOEA/D-DRA to the same test problems. It shows that ESOEA/DE performs superior to MOEA/D-DRA in 8 out of 10 cases and performs superior or equivalent to ENS-MOEA/D in 6 out of 10 cases. For supporting these results, the Pareto-fronts of the problems as obtained in the median cases by ESOEA/DE are shown in Fig. 8. Except for UF1 and UF3, these Pareto-fronts bear more resemblance to the true Pareto-fronts as compared to the ones reported in Ref. [64]. This superior performance of ESOEA over ENS-MOEA/D and MOEA/D-DRA is because ESOEA exhibits adaptability in terms of both reproduction operators (SaNSDE [62]) as well as sub-population sizes. These experiments establish the versatility of ESOEA/DE for addressing MOO problems.

### 4.5. Comparison of ESOEA/DE with various categories of MOEAs

From the four categories of MOEAs mentioned in Section 1, the following representative algorithms are chosen: NSGA-II [11] (Pareto-dominance based MOEA), MOEA/D [32] (decomposition based MOEA), HypE [27] (indicator based MOEA) and $\alpha$-DEMO [10] (objective reduction based MOEA). The performance of ESOEA/DE is compared with these algorithms on 10 and 20-objective DTLZ problems in terms of convergence metric (Table 6) and hypervolume indicator (Table 7). Hypervolume indicator is realized with $|H| = 10000$ and $F_{ref} = [3, \overset{M \text{ times}}{\cdots}, 3]$ as done in Ref. [10]. As ESOEA/DE is a DE-based MOEA, its compar-

**Table 7**
Hypervolume values of ESOEA/DE and various other kinds of evolutionary algorithms from 30 independent runs for DTLZ problems.

| Problems | $M$ | NSGA-II | MOEA/D | HypE | DEMO | $\alpha$-DEMO-r | ESOEA/DE |
|---|---|---|---|---|---|---|---|
| DTLZ1 | 10 | 0.0044 ± 0.0016(+) | 0.8132 ± 0.0984(+) | 0.0000 ± 0.0000(+) | 0.0000 ± 0.0000(+) | 0.9536 ± 0.0166(+) | **0.9970 ± 0.0015** |
| | 20 | 0.0000 ± 0.0000(+) | 0.7233 ± 0.1172(+) | 0.0000 ± 0.0000(+) | 0.0000 ± 0.0000(+) | 0.9779 ± 0.0176(+) | **0.9903 ± 0.0016** |
| DTLZ2 | 10 | 0.8399 ± 0.0079(+) | **1.0000 ± 0.0000**(≈) | 0.9514 ± 0.0034(+) | 0.8863 ± 0.0059(+) | 0.9110 ± 0.0155(+) | **1.0000 ± 0.0000** |
| | 20 | 0.8280 ± 0.0070(+) | **1.0000 ± 0.0000**(≈) | 0.9372 ± 0.0019(+) | 0.8487 ± 0.0059(+) | 0.9560 ± 0.0159(+) | **1.0000 ± 0.0000** |
| DTLZ3 | 10 | 0.0000 ± 0.0000(+) | 0.0235 ± 0.0188(+) | 0.0000 ± 0.0000(+) | 0.0000 ± 0.0000(+) | 0.1269 ± 0.0021(+) | **0.9997 ± 0.0002** |
| | 20 | 0.0000 ± 0.0000(+) | 0.0301 ± 0.0031(+) | 0.0000 ± 0.0000(+) | 0.0000 ± 0.0000(+) | 0.3213 ± 0.0055(+) | **0.9985 ± 0.0007** |
| DTLZ4 | 10 | 0.9765 ± 0.0056(+) | **1.0000 ± 0.0000**(≈) | 0.8741 ± 0.0169(+) | 0.9956 ± 0.0012(+) | 0.9700 ± 0.0155(+) | **1.0000 ± 0.0000** |
| | 20 | 0.9914 ± 0.0030(+) | **1.0000 ± 0.0000**(≈) | 0.8963 ± 0.0103(+) | 0.9829 ± 0.0111(+) | 0.9768 ± 0.0158(+) | **1.0000 ± 0.0000** |
| DTLZ7 | 10 | 0.0000 ± 0.0000(≈) | 0.0000 ± 0.0000(≈) | 0.0000 ± 0.0000(≈) | 0.0000 ± 0.0000(≈) | **0.0116 ± 0.0002**(−) | 0.0000 ± 0.0000 |
| | 20 | 0.0000 ± 0.0000(≈) | 0.0000 ± 0.0000(≈) | 0.0000 ± 0.0000(≈) | 0.0000 ± 0.0000(≈) | **0.0103 ± 0.0002**(−) | 0.0000 ± 0.0000 |
| +/ − / ≈ | | 8/0/2 | 4/0/6 | 8/0/2 | 8/0/2 | 8/2/0 | |

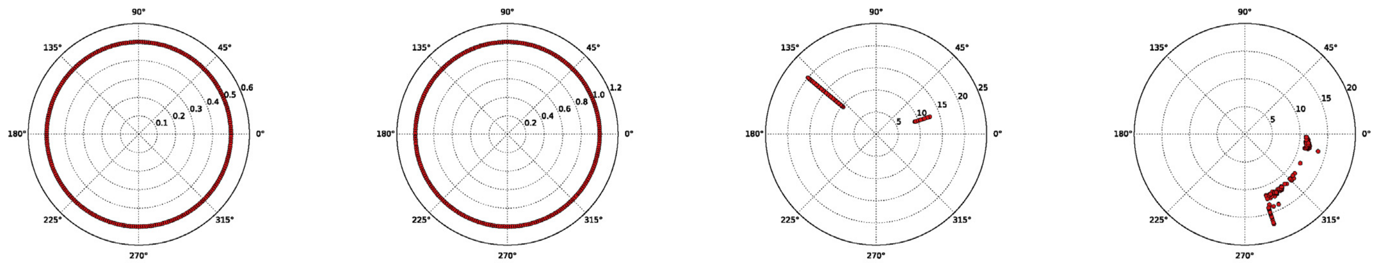

(a) DTLZ1(10) (b) DTLZ4(10) (c) DTLZ7(10) (d) WFG1(10)

**Fig. 9.** Pareto-fronts obtained through ESOEA/DE for 10-objective test problems.

ison is also done with DEMO [66]. These competitor algorithms are set as per the specifications in Ref. [10] and for $\alpha$-DEMO-revised [10] (mentioned as $\alpha$-DEMO-r, hereafter), $\alpha$ corresponding to the best performance is considered. In support of the values obtained in Tables 6 and 7, some *PF*s are visualized in Fig. 9 using the spherical coordinates method, proposed in Ref. [61].

From Table 6 (where ESOEA/DE is the best or second-best performing MOEA in 9 out of 10 cases) and Fig. 9, the following observations are noted for performance in terms of convergence metric.

- For unimodal problems (like DTLZ2 and DTLZ4), although ESOEA/DE has good performance, $\alpha$-DEMO-r has better performance than ESOEA/DE. This can be attributed to the better selection pressure for the reduced objective problem. Moreover, DTLZ4 has a biased density of solutions towards $f_M - f_1$ plane due to meta-variable mapping [56]. The adaptive feedback strategy of ESOEA/DE helps in the exploration of the search space for such problems. Thus, the performance of ESOEA/DE is not far behind.
- For multi-modal problems (like DTLZ1 and DTLZ3), the performance of ESOEA/DE is better than most of the MOEAs which can be attributed to the fact that NSDE part of SaNSDE is effective in escaping from local minima [62].
- For DTLZ7 with disconnected Pareto-front (Fig. 9c shows two Pareto-optimal patches), ESOEA/DE outperforms other competitor algorithms. The reasons for this improved performance is because ESOEA/DE, being a reference direction based approach with adaptive feedback strategy, ensures the proper balance of exploration and exploitation of the search space.
- Based on convergence, $\alpha$-DEMO-r and ESOEA/DE tie. The better performance of $\alpha$-DEMO-r and ESOEA/DE is due to the adoption of regulated elitism that avoids premature termination of MaOO algorithms for problems with a large number of objectives.

From Table 7 (where ESOEA/DE is the best performing MOEA in 8 out of 10 cases) and Fig. 9, the following observations are noted for performance in terms of hypervolume indicator.

- Being decomposition algorithms, MOEA/D and ESOEA/DE has embedded diversity enforcing mechanism. This leads to the superior hypervolume for the Pareto-fronts resulting from these algorithms.
- It can be noted from Fig. 9c, that even for 10 objectives, *PF* of DTLZ7 is outside the hyper-rectangle considered for evaluation of hypervolume indicator. Hence, the value of hypervolume indicator is zero in most of these test cases, except for $\alpha$-DEMO-r. The MaOO algorithm of $\alpha$-DEMO-r operates on reduced objective set and hence, is able to discover a few points within the hyper-rectangle concerned for calculating the hypervolume indicator.
- Based on hypervolume, ESOEA/DE is the clear winner among these six competitor algorithms.

Thus, ESOEA/DE has superior performance on a variety of problem characteristics as compared to popular MOO and MaOO algorithms from various categories of MOEAs.

### 4.6. Comparison of ESOEA/DE with MOEAs using reference vectors

As ESOEA/DE is a reference vector based approach, it is only fair to compare its performance with other contemporary reference vector based approaches such as NSGA-III [38], MOEA/DD [15], RVEA [48] and AR-MOEA [47] which are set up as per the specifications in Ref. [47]. The comparison is done on normalized *PF* between ideal and nadir points in terms of hypervolume indicator with $|H| = 1,000,000$ and $F_{ref} = [1.1, \overset{M \text{ times}}{\cdots}, 1.1]$. As noted in Table 8, ESOEA/DE outperforms these competitor algorithms in 9 out of 14 test cases, followed by AR-MOEA which shows superior performance in 4 out of 14 test cases. The *PF*s for 10-objective test problems have been illustrated in Fig. 9. The following observations are made from Table 8:

**Table 8**
Hypervolume values of reference vector associated MaOO algorithms from 30 independent runs for 5- and 10-objective problems with regular and irregular Pareto-fronts.

| Problems | $M$ | NSGA-III | MOEA/DD | RVEA | AR-MOEA | ESOEA/DE |
|---|---|---|---|---|---|---|
| DTLZ1 | 5 | 9.7456E-01 ± 4.86E-04(−) | 9.7487E-01 ± 1.94E-04(−) | 9.7478E-01 ± 3.14E-04(−) | **9.7492E-01 ± 1.53E-04**(−) | 9.7113E-01 ± 1.05E-03 |
| | 10 | 9.8390E-01 ± 4.66E-02(−) | 9.9957E-01 ± 4.55E-05(−) | 9.9967E-01 ± 2.82E-05(−) | **9.9971E-01 ± 8.84E-06**(−) | 9.1338E-01 ± 9.48E-02 |
| DTLZ2 | 5 | 7.9035E-01 ± 8.70E-04(+) | 7.9294E-01 ± 5.49E-02(≈) | 7.9209E-01 ± 6.51E-04(+) | 7.9047E-01 ± 8.44E-04(+) | **8.1198E-01 ± 1.21E-03** |
| | 10 | 9.4923E-01 ± 3.10E-02(+) | 9.6735E-01 ± 2.41E-04(+) | 9.6751E-01 ± 2.27E-04(+) | 9.6432E-01 ± 8.26E-04(+) | **9.6852E-01 ± 4.00E-04** |
| DTLZ3 | 5 | 5.9177E-01 ± 2.97E-01(+) | 7.7880E-01 ± 1.20E-02(+) | 7.3843E-01 ± 7.61E-02(+) | 7.7240E-01 ± 7.36E-03(+) | **8.5123E-01 ± 8.62E-03** |
| | 10 | 3.8532E-01 ± 3.38E-01(+) | 9.6669E-01 ± 2.00E-03(−) | 9.6065E-01 ± 6.15E-03(−) | **9.6723E-01 ± 2.93E-03**(−) | 8.8142E-01 ± 8.66E-02 |
| DTLZ4 | 5 | 7.8203E-01 ± 2.89E-02(≈) | 7.9366E-01 ± 5.01E-04(+) | 7.9307E-01 ± 4.99E-04(+) | 7.9077E-01 ± 6.88E-04(+) | **8.0225E-01 ± 9.41E-04** |
| | 10 | 9.6625E-01 ± 9.90E-04(+) | 9.6837E-01 ± 3.23E-03(≈) | 9.6964E-01 ± 2.83E-04(≈) | 9.6902E-01 ± 5.57E-04(≈) | **9.6966E-01 ± 8.06E-04** |
| DTLZ7 | 5 | 2.4167E-01 ± 4.33E-03(+) | 9.0909E-02 ± 4.94E-07(+) | 2.0007E-01 ± 9.91E-03(+) | 2.3599E-01 ± 2.48E-03(+) | **5.0892E-01 ± 1.54E-02** |
| | 10 | 1.9584E-01 ± 1.26E-02(+) | 1.1971E-03 ± 3.11E-04(+) | 1.4380E-01 ± 1.51E-02(+) | 1.4646E-01 ± 7.03E-03(+) | **6.0554E-01 ± 3.05E-02** |
| WFG1 | 5 | 7.8837E-01 ± 3.33E-02(+) | 7.7075E-01 ± 5.71E-02(+) | 8.6621E-01 ± 4.04E-02(+) | 9.0787E-01 ± 2.65E-02(+) | **9.5295E-01 ± 6.42E-03** |
| | 10 | 7.0682E-01 ± 4.79E-02(+) | 9.8947E-01 ± 2.24E-02(≈) | 9.8712E-01 ± 2.83E-02(+) | 9.4718E-01 ± 3.69E-02(+) | **9.9064E-01 ± 1.74E-03** |
| WFG2 | 5 | 9.9246E-01 ± 1.19E-03(−) | 9.6933E-01 ± 4.70E-03(−) | 9.8809E-01 ± 1.99E-03(−) | **9.9469E-01 ± 5.81E-04**(−) | 7.0163E-01 ± 3.58E-02 |
| | 10 | **9.9671E-01 ± 1.69E-03**(−) | 9.6285E-01 ± 6.50E-03(−) | 9.8615E-01 ± 3.22E-03(−) | 9.9508E-01 ± 1.06E-03(−) | 7.3139E-01 ± 2.75E-02 |
| +/−/≈ | | 9/4/1 | 6/5/3 | 8/5/1 | 8/5/1 | |

**Table 9**
Mean IGD values of recent adaptive MaOO algorithms over 30 independent runs for multimodal problems with regular Pareto-fronts.

| Problems | $M$ | A-NSGA-III | RVEA* | AR-MOEA | ESOEA/DE |
|---|---|---|---|---|---|
| DTLZ1 | 3 | 2.3434E-02(+) | 2.8841E-02(+) | 1.8931E-02(+) | **1.1561E-02** |
| | 5 | 6.3446E-02(+) | 7.1247E-02(+) | 6.2861E-02(+) | **4.0492E-02** |
| | 10 | 1.7341E-01(−) | 2.5566E-01(−) | **1.4292E-01**(−) | 4.0598E-01 |
| DTLZ3 | 3 | 6.8590E-02(+) | 7.2553E-02(+) | **5.0276E-02**(−) | 5.9847E-02 |
| | 5 | 2.0753E-01(+) | 2.8049E-01(+) | 1.9531E-01(+) | **1.1701E-01** |
| | 10 | 2.0584E+00(+) | 6.9093E-01(−) | **4.9583E-01**(−) | 1.2617E+00 |
| +/ − / ≈ | | 5/1/0 | 4/2/0 | 3/3/0 | |

- Better performance of ESOEA/DE than NSGA-III can be attributed to its regulated elitist selection. NSGA-III [38] being a Pareto-dominance approach suffers from dominance resistance. Also, adaptive feedback of ESOEA/DE is beneficial than the association scheme of NSGA-III (Section 3.6).
- Adaptive feedback of ESOEA/DE also leads to its better performance for problems like DTLZ7 (disconnected *PF*) and WFG1 (sharp-tailed *PF*) as compared to the strategies of MOEA/DD which yields better performance for problems like DTLZ1 and DTLZ3 (multi-modal but regular *PF*).
- ESOEA/DE outperforms RVEA [48] as the former performs mating in a local neighborhood which helps in better exploitation and in keeping the global population size in check, with an increase in $M$ [15].
- Unlike ESOEA/DE, AR-MOEA adapts the reference vectors based on IGD-NS. However, this leads to difficulty in exploring problems with difficult regions such as DTLZ4 (biased density).

For a deeper analysis of the adaptive tendency of ESOEA/DE, its performance is compared specifically with reference vector adaptation based MaOO algorithms viz. A-NSGA-III [50], RVEA∗ [48] and AR-MOEA [47] in Table 9 using IGD values from DTLZ1 and DTLZ3 test problems. These competitor algorithms are set as in Ref. [47]. It can be noted from Table 9 that ESOEA/DE clearly outperforms A-NSGA-III and RVEA∗. This is because the adaptive strategies of A-NSGA-III and RVEA∗ have been developed specifically for problems with irregular *PF*. However, on the basis of IGD, ESOEA/DE tie with AR-MOEA for addressing MaOO problems with regular *PF*.

### 4.7. Effectiveness of components of ESOEA/DE

For investigating the effectiveness of various components of the proposed approach, the following experiments are performed where the basic framework of ESOEA/DE is kept intact, except changing only one of the components:

1. *Experiment-I*: Using DE/rand/1/bin [46,67] instead of SaNSDE
2. *Experiment-II*: Using non-dominated sorting [11] with crowding distance (Eq. (12)) based secondary selection (Section 3.5.1) instead of the selection scheme proposed in Section 3.5.2
3. *Experiment-III*: Using $\theta = 0$ (weighted sum) instead of PBI for fitness transformation in Eq. (10)
4. *Experiment-IV*: Using weight distribution based on maximization of minimum pair-wise distance instead of Das and Dennis's two-layered approach [49] (details of this approach are elaborated in the supplementary material which is available at http://worksupplements.droppages.com/esoea)

These experiments are performed on both multi- and many-objective test problems and their performance are noted in Table 10 in terms

**Table 10**
Hypervolume values of experiments on ESOEA/DE from 30 independent runs for 3-, 5-, 10- and 20-objective problems with regular and irregular Pareto-fronts.

| Problems | $M$ | ESOEA/DE | Experiment-I | Experiment-II | Experiment-III | Experiment-IV |
|---|---|---|---|---|---|---|
| DTLZ1 | 3 | 8.5453E-01 ± 2.99E-03 | 8.4154E-01 ± 1.44E-03 (+) | **8.5658E-01 ± 6.08E-04** (−) | 8.1774E-01 ± 2.72E-02 (+) | 7.9633E-01 ± 1.58E-03 (+) |
| DTLZ2 | 3 | 5.7467E-01 ± 2.37E-03 | 5.6276E-01 ± 6.51E-03 (+) | **5.8463E-01 ± 5.37E-03** (−) | 5.7097E-01 ± 2.93E-03 (+) | 5.1058E-01 ± 2.10E-03 (+) |
| DTLZ3 | 3 | 5.6074E-01 ± 1.10E-03 | 5.5885E-01 ± 1.11E-03 (+) | **5.8437E-01 ± 1.11E-03** (−) | 5.6102E-01 ± 2.94E-04 (≈) | 5.0282E-01 ± 1.41E-03 (+) |
| DTLZ4 | 3 | 5.6318E-01 ± 1.38E-03 | 5.6136E-01 ± 1.90E-03 (+) | **5.8660E-01 ± 6.17E-04** (−) | 5.5706E-01 ± 2.68E-03 (+) | 5.0291E-01 ± 1.04E-03 (+) |
| DTLZ7 | 3 | **5.7580E-01 ± 5.11E-02** | 4.4063E-01 ± 3.03E-03 (+) | 5.3227E-01 ± 3.09E-02 (+) | 5.5827E-01 ± 8.67E-02 (≈) | 4.4002E-01 ± 9.75E-03 (+) |
| WFG1 | 3 | **8.0581E-01 ± 3.98E-03** | 7.8667E-01 ± 1.85E-03 (+) | 7.6349E-01 ± 4.67E-02 (+) | 7.5286E-01 ± 2.99E-02 (+) | 7.3019E-01 ± 2.67E-02 (+) |
| WFG2 | 3 | **6.9209E-01 ± 1.47E-02** | 6.6852E-01 ± 6.03E-04 (+) | 6.8132E-01 ± 1.26E-02 (≈) | 6.5564E-01 ± 1.40E-02 (+) | 6.1144E-01 ± 1.38E-02 (+) |
| DTLZ1 | 5 | 9.7113E-01 ± 1.05E-03 | 9.7427E-01 ± 2.27E-04 (−) | 9.7014E-01 ± 1.54E-03 (≈) | **9.8447E-01 ± 4.69E-04** (−) | 8.5232E-01 ± 1.03E-03 (+) |
| DTLZ2 | 5 | **8.1198E-01 ± 1.21E-03** | 8.0876E-01 ± 3.48E-03 (+) | 8.0901E-01 ± 3.70E-03 (+) | 8.0099E-01 ± 3.46E-03 (+) | 6.8135E-01 ± 1.25E-03 (+) |
| DTLZ3 | 5 | **8.5123E-01 ± 8.62E-03** | 8.0531E-01 ± 2.86E-03 (+) | 8.4474E-01 ± 1.91E-02 (≈) | 8.4419E-01 ± 2.49E-02 (≈) | 7.1841E-01 ± 9.03E-03 (+) |
| DTLZ4 | 5 | 8.0225E-01 ± 9.41E-04 | **8.0710E-01 ± 1.23E-03** (−) | 8.0046E-01 ± 6.19E-04 (+) | 7.9584E-01 ± 4.19E-04 (+) | 6.7313E-01 ± 2.12E-03 (+) |
| DTLZ7 | 5 | 5.0892E-01 ± 1.54E-02 | 5.3167E-01 ± 1.37E-02 (−) | **5.6352E-01 ± 2.68E-02** (−) | 5.5237E-01 ± 3.28E-02 (−) | 3.9291E-01 ± 2.35E-02 (+) |
| WFG1 | 5 | **9.5295E-01 ± 6.42E-03** | 9.4304E-01 ± 1.89E-03 (+) | 9.3726E-01 ± 5.45E-03 (+) | 9.3512E-01 ± 5.33E-03 (+) | 5.1293E-01 ± 1.64E-02 (+) |
| WFG2 | 5 | 7.0163E-01 ± 3.58E-02 | 6.9669E-01 ± 1.01E-03 (≈) | 6.4977E-01 ± 1.88E-02 (+) | 6.6672E-01 ± 1.07E-02 (+) | **8.0880E-01 ± 2.31E-02** (−) |
| DTLZ1 | 10 | 9.1338E-01 ± 9.48E-02 | **9.9814E-01 ± 2.92E-04** (−) | 8.9365E-01 ± 5.44E-02 (≈) | 9.6804E-01 ± 3.19E-03 (−) | 7.4837E-01 ± 1.41E-01 (+) |
| DTLZ2 | 10 | **9.6852E-01 ± 4.00E-04** | 9.1965E-01 ± 5.33E-04 (+) | 9.2339E-01 ± 1.77E-03 (+) | 9.6504E-01 ± 5.84E-04 (+) | 7.3232E-01 ± 2.09E-03 (+) |
| DTLZ3 | 10 | **8.8142E-01 ± 8.66E-02** | 7.7287E-01 ± 6.07E-04 (+) | 6.9587E-01 ± 1.26E-01 (+) | 8.3545E-01 ± 1.16E-02 (+) | 8.8016E-01 ± 3.24E-02 (≈) |
| DTLZ4 | 10 | **9.6966E-01 ± 8.06E-04** | 8.7187E-01 ± 4.16E-04 (+) | 8.7648E-01 ± 6.55E-04 (+) | 9.6828E-01 ± 2.99E-04 (+) | 7.2930E-01 ± 3.46E-03 (+) |
| DTLZ7 | 10 | 6.0554E-01 ± 3.05E-02 | 6.9478E-01 ± 1.58E-02 (−) | **7.7617E-01 ± 3.34E-02** (−) | 5.6036E-01 ± 1.47E-01 (≈) | 6.2205E-01 ± 1.79E-02 (≈) |
| WFG1 | 10 | **9.9064E-01 ± 1.74E-03** | 9.8725E-01 ± 1.94E-03 (+) | 9.0984E-01 ± 2.47E-03 (+) | 9.2766E-01 ± 9.73E-03 (+) | 8.4420E-01 ± 1.62E-02 (+) |
| WFG2 | 10 | **7.3139E-01 ± 2.75E-02** | 6.7190E-01 ± 6.31E-03 (+) | 6.4810E-01 ± 1.66E-02 (+) | 6.2490E-01 ± 2.18E-02 (+) | 5.9579E-01 ± 4.73E-02 (+) |
| DTLZ1 | 20 | 8.1368E-01 ± 1.05E-01 | 9.6994E-01 ± 6.52E-03 (−) | 8.5046E-01 ± 1.10E-02 (≈) | 9.3120E-01 ± 4.92E-03 (−) | **9.9752E-01 ± 4.31E-04** (−) |
| DTLZ2 | 20 | **9.8335E-01 ± 1.66E-02** | 9.6377E-01 ± 8.89E-04 (+) | 9.1597E-01 ± 1.89E-02 (+) | 9.6395E-01 ± 3.19E-03 (+) | 8.5250E-01 ± 6.49E-03 (+) |
| DTLZ3 | 20 | **7.5869E-01 ± 1.01E-01** | 6.7534E-01 ± 2.45E-02 (+) | 5.7603E-01 ± 1.77E-01 (+) | 6.8463E-01 ± 2.69E-03 (+) | 7.1100E-01 ± 7.37E-02 (≈) |
| DTLZ4 | 20 | **9.9875E-01 ± 7.68E-05** | 9.9871E-01 ± 6.58E-05 (≈) | 9.9456E-01 ± 1.12E-03 (+) | 9.9834E-01 ± 2.28E-04 (+) | 9.7615E-01 ± 1.17E-05 (+) |
| DTLZ7 | 20 | 8.0038E-01 ± 6.11E-02 | 3.1698E-01 ± 7.78E-02 (+) | **8.4948E-01 ± 1.15E-02** (−) | 6.4741E-01 ± 1.97E-01 (+) | 5.2040E-01 ± 7.65E-02 (+) |
| WFG1 | 20 | 7.5766E-01 ± 2.76E-02 | **7.8495E-01 ± 4.29E-03** (−) | 7.1659E-01 ± 1.07E-02 (+) | 7.7598E-01 ± 8.50E-03 (≈) | 6.6224E-01 ± 3.88E-02 (+) |
| WFG2 | 20 | 6.2019E-01 ± 1.16E-02 | 5.8943E-01 ± 4.45E-02 (+) | 6.0747E-01 ± 1.10E-02 (+) | **6.3564E-01 ± 1.02E-02** (−) | 6.0435E-01 ± 3.71E-02 (≈) |
| +/ − / ≈ | | | 19/7/2 | 16/7/5 | 18/5/5 | 22/2/4 |

of hypervolume indicator from normalized *PF* between ideal and nadir points with $|H| = 1,000,000$ and $F_{ref} = [1.1, \overset{M \text{ times}}{\cdots}, 1.1]$. From Table 10, it is observed that ESOEA/DE (the proposed framework) performs best or second-best in 21 out of 28 test cases as compared to other the other experimental frameworks. Even for 3-objective DTLZ3 and 20-objective WFG1 problems, the hypervolume value of ESOEA/DE is not significantly different from the second-best value.

A more thorough inspection of Table 10 yields the following insights:

- ESOEA/DE performs better or equivalent to Experiment-I in 21 out of 28 test cases as using SaNSDE (ESOEA/DE) instead of classical DE (Experiment-I) aids in local adaptability to problem characteristics. Also, Experiment-I shows the second highest number of best or second-best performances, supporting the efficacy of other modules used in ESOEA/DE.
- For 3-objective DTLZ1, DTLZ2, DTLZ3 and DTLZ4 problems, the framework of Experiment-II performs better than the proposed ESOEA/DE framework. As the number of objectives increases, the effectiveness of non-dominated sorting with crowding distance based selection (Experiment-II) fades away in comparison to the regulated elitism scheme of ESOEA/DE.
- ESOEA/DE performs significantly better or equivalent to Experiment-III in 23 out of 28 test cases as using PBI (ESOEA/DE) instead of weighted sum (Experiment-III) presents a better trade-off between convergence and diversity.
- The alternate weight distribution scheme (Experiment-IV) gives poorer result than ESOEA/DE for problems with a low number of objectives. However, it performs significantly better or equivalent to ESOEA/DE in 5 test cases for problems with a high number of objectives (10- and 20-objective). This is because for such problems there are few intermediate weight vectors (inside layer) which hampers the diversity of resulting Pareto-front.

These observations demonstrate that the combination of modules of ESOEA/DE is significantly better than the usual existing modules.

Thus, from all the results presented in this manuscript, it can be concluded that the proposed algorithmic framework (ESOEA/DE) is efficient and versatile for addressing a variety of challenging MaOO problems.

## 5. Conclusion

This work presents a many-objective optimization (MaOO) framework that uses an ensemble of single objective Differential Evolution with Self-adaptive Neighborhood Search (SaNSDE) to perform optimization. Penalty-based boundary intersection (PBI) scalarization assists in transforming a MaOO problem into multiple single objective optimization sub-problems. The feedback step imparts the adaptive quality to the framework by negatively correlating the subpopulation sizes for each optimizer with respect to their contribution towards the population for the next generation. Besides the adaptability to problem requirement, a faster randomized candidate association, and a regulated elitism scheme to avoid the saturation problem of MaOO, are its other novel features. Results exhibit the robustness of ESOEA/DE by presenting good convergence and superior diversity with respect to problem features like different modalities, biased density of solutions, disconnected Pareto-fronts, Pareto-fronts with sharp-tails, imbalance difficulties and difficulties associated with variable linkage.

The following research directions can be considered for further investigations of the proposed experimental framework:

1. Although the performance of the proposed framework has been investigated on DTLZ, WFG, IMB and CEC 2009 test suites, yet there are several recent problems based on complexities like objective scalability, multi-modality, disconnectedness, and bias as defined in Ref. [68]. Also, difficulties like objective scalability, complicated Pareto set, bias, disconnection, and degeneracy are seen in the problems, defined in Ref. [69]. Analyzing the performance of the proposed framework on these new test problems possesses itself as a potential future work.
2. Application on real-life problems is necessary for practical validation of the proposed framework.
3. An advantage of this simple adaptive MaOO framework is its inherent parallelism that should be further exploited to obtain much faster results.
4. The feedback strategy can be modified for regulating the reference direction vectors or introducing time-sensitive weight vectors to address problems with a dynamic landscape [1].
5. There are very limited studies on large-scale MaOO problems [1]. As a preliminary work, large-scale SOEA can be directly integrated with the proposed ESOEA framework to yield an extended framework for large scale MaOO problems.
6. As ensemble approaches [70] help to generalize better by introducing more randomness [71], such approaches can be explored to combine subpopulation from different optimizers which can incorporate decision maker's preferences.

Thus, further studies and extensions of the proposed adaptive ESOEA framework for MaOO problems along the above-mentioned directions are open for future research.

### Acknowledgement

This study has been supported by Indian Statistical Institute, India.

### References

[1] C.A.C. Coello, Recent results and open problems in evolutionary multiobjective optimization, in: C. Martín-Vide, R. Neruda, M.A. Vega-Rodríguez (Eds.), Theory and Practice of Natural Computing, Springer International Publishing, Cham, 2017, pp. 3–21.

[2] H. Ishibuchi, N. Tsukamoto, Y. Nojima, Evolutionary many-objective optimization: a short review, in: Evolutionary Computation, 2008. CEC 2008. (IEEE World Congress on Computational Intelligence). IEEE Congress on, 2008, pp. 2419–2426, https://doi.org/10.1109/CEC.2008.4631121.

[3] M. Pal, S. Saha, S. Bandyopadhyay, Clustering based online automatic objective reduction to aid many-objective optimization, in: 2016 IEEE Congress on Evolutionary Computation (CEC), IEEE, 2016, pp. 1131–1138, https://doi.org/10.1109/CEC.2016.7743915.

[4] F. Neri, C. Cotta, Memetic algorithms and memetic computing optimization: a literature review, Swarm Evolut. Comput. 2 (2012) 1–14. https://doi.org/10.1016/j.swevo.2011.11.003.

[5] A. Zhou, B.-Y. Qu, H. Li, S.-Z. Zhao, P.N. Suganthan, Q. Zhang, Multiobjective evolutionary algorithms: a survey of the state of the art, Swarm Evolut. Comput. 1 (1) (2011) 32–49.

[6] B.A. Attea, W.A. Hariz, M.F. Abdulhalim, Improving the performance of evolutionary multi-objective co-clustering models for community detection in complex social networks, Swarm Evolut. Comput. 26 (2016) 137–156. https://doi.org/10.1016/j.swevo.2015.09.003.

[7] K. Elsayed, C. Lacor, CFD modeling and multi-objective optimization of cyclone geometry using desirability function, artificial neural networks and genetic algorithms, Appl. Math. Model. 37 (8) (2013) 5680–5704.

[8] M. Pal, S. Bandyopadhyay, Many-objective feature selection for motor imagery EEG signals using differential evolution and support vector machine, in: IEEE International Conference on Microelectronics, Computing and Communication, MicroCom 2016, 2016, pp. 1–6.

[9] A. García-Nájera, A. López-Jaimes, An investigation into many-objective optimization on combinatorial problems: analyzing the pickup and delivery problem, Swarm Evolut. Comput. 38 (2018) 218–230.

[10] S. Bandyopadhyay, A. Mukherjee, An algorithm for many-objective optimization with reduced objective computations: a study in differential evolution, Evolut. Comput., IEEE Trans. 19 (3) (2015) 400–413.

[11] K. Deb, A. Pratap, S. Agarwal, T. Meyarivan, A fast and elitist multiobjective genetic algorithm: NSGA-II, Evolut. Comput., IEEE Trans. 6 (2) (2002) 182–197, https://doi.org/10.1109/4235.996017.

[12] E. Zitzler, M. Laumanns, L. Thiele, SPEA2: improving the strength pareto evolutionary algorithm for multiobjective optimization, Evolut. Methods Design, Optim. Control (2002) 95–100.

[13] D.W. Corne, N.R. Jerram, J.D. Knowles, M.J. Oates, PESA-II: region-based selection in evolutionary multiobjective optimization, in: Proceedings of the 3rd Annual Conference on Genetic and Evolutionary Computation, Morgan Kaufmann Publishers Inc., 2001, pp. 283–290.

[14] M. Pal, S. Saha, S. Bandyopadhyay, DECOR: differential evolution using clustering based objective reduction for many-objective optimization, Inf. Sci. 423 (2018) 200–218. https://doi.org/10.1016/j.ins.2017.09.051.
[15] K. Li, K. Deb, Q. Zhang, S. Kwong, An evolutionary many-objective optimization algorithm based on dominance and decomposition, IEEE Trans. Evol. Comput. 19 (5) (2015) 694–716.
[16] R.C. Purshouse, P.J. Fleming, On the evolutionary optimization of many conflicting objectives, IEEE Trans. Evol. Comput. 11 (6) (2007) 770–784.
[17] K. Deb, M. Mohan, S. Mishra, Evaluating the $\epsilon$-domination based multi-objective evolutionary algorithm for a quick computation of pareto-optimal solutions, Evol. Comput. 13 (4) (2005) 501–525.
[18] Y. Yuan, X. Hua, W. Bo, Y. Xin, A new dominance relation-based evolutionary algorithm for many-objective optimization, IEEE Trans. Evol. Comput. 20 (1) (2016) 16–37, https://doi.org/10.1109/TEVC.2015.2420112.
[19] N. Drechsler, R. Drechsler, B. Becker, Multi-objective optimisation based on relation favour, in: Evolutionary Multi-Criterion Optimization, Springer, 2001, pp. 154–166.
[20] Z. He, G.G. Yen, J. Zhang, Fuzzy-based pareto optimality for many-objective evolutionary algorithms, Evolut. Comput., IEEE Trans. 18 (2) (2014) 269–285, https://doi.org/10.1109/TEVC.2013.2258025.
[21] S. Yang, M. Li, X. Liu, J. Zheng, A grid-based evolutionary algorithm for many-objective optimization, IEEE Trans. Evol. Comput. 17 (5) (2013) 721–736.
[22] X. Zhang, Y. Tian, Y. Jin, A knee point-driven evolutionary algorithm for many-objective optimization, IEEE Trans. Evol. Comput. 19 (6) (2015) 761–776.
[23] E. Zitzler, S. Künzli, Indicator-based selection in multiobjective search, in: International Conference on Parallel Problem Solving from Nature, Springer, 2004, pp. 832–842.
[24] N. Beume, B. Naujoks, M. Emmerich, SMS-EMOA: multiobjective selection based on dominated hypervolume, Eur. J. Oper. Res. 181 (3) (2007) 1653–1669.
[25] A. Menchaca-Mendez, C.A.C. Coello, GDE-MOEA: a new moea based on the generational distance indicator and $\epsilon$-dominance, in: Evolutionary Computation (CEC), 2015 IEEE Congress on, IEEE, 2015, pp. 947–955.
[26] R. Hernández Gómez, C.A. Coello Coello, Improved metaheuristic based on the R2 indicator for many-objective optimization, in: Proceedings of the 2015 Annual Conference on Genetic and Evolutionary Computation, ACM, 2015, pp. 679–686.
[27] J. Bader, E. Zitzler, HypE: an algorithm for fast hypervolume-based many-objective optimization, Evol. Comput. 19 (1) (2011) 45–76.
[28] A.P. Guerreiro, C.M. Fonseca, Hypervolume sharpe-ratio indicator: formalization and first theoretical results, in: J. Handl, E. Hart, P.R. Lewis, M. López-Ibáñez, G. Ochoa, B. Paechter (Eds.), Parallel Problem Solving from Nature – PPSN XIV, Springer International Publishing, Cham, 2016, pp. 814–823.
[29] D.K. Saxena, J.A. Duro, A. Tiwari, K. Deb, Z. Qingfu, Objective reduction in many-objective optimization: linear and nonlinear algorithms, Evolut. Comput., IEEE Trans. 17 (1) (2013) 77–99, https://doi.org/10.1109/TEVC.2012.2185847.
[30] A.L. Jaimes, C.A.C. Coello, D. Chakraborty, Objective reduction using a feature selection technique, in: Proceedings of the 10th Annual Conference on Genetic and Evolutionary Computation, ACM, 2008, pp. 673–680.
[31] A.L. Jaimes, C.A.C. Coello, J.E.U. Barrientos, Online objective reduction to deal with many-objective problems, in: Evolutionary Multi-Criterion Optimization, Springer, 2009, pp. 423–437.
[32] Z. Qingfu, L. Hui, MOEA/D: a multiobjective evolutionary algorithm based on decomposition, Evolut. Comput., IEEE Trans. 11 (6) (2007) 712–731, https://doi.org/10.1109/TEVC.2007.892759.
[33] Y. Jin, T. Okabe, B. Sendho, Adapting weighted aggregation for multiobjective evolution strategies, in: E. Zitzler, L. Thiele, K. Deb, C.A. Coello Coello, D. Corne (Eds.), Evolutionary Multi-Criterion Optimization, Springer Berlin Heidelberg, Berlin, Heidelberg, 2001, pp. 96–110.
[34] E.J. Hughes, MSOPS-II: a general-purpose many-objective optimiser, in: Evolutionary Computation, 2007. CEC 2007. IEEE Congress on, IEEE, 2007, pp. 3944–3951.
[35] A. Jaszkiewicz, Genetic local search for multi-objective combinatorial optimization, Eur. J. Oper. Res. 137 (1) (2002) 50–71.
[36] H.-L. Liu, F. Gu, Q. Zhang, Decomposition of a multiobjective optimization problem into a number of simple multiobjective subproblems, IEEE Trans. Evol. Comput. 18 (3) (2014) 450–455.
[37] H.-L. Liu, L. Chen, K. Deb, E.D. Goodman, Investigating the effect of imbalance between convergence and diversity in evolutionary multiobjective algorithms, IEEE Trans. Evol. Comput. 21 (3) (2017) 408–425.
[38] K. Deb, H. Jain, An evolutionary many-objective optimization algorithm using reference-point-based nondominated sorting approach, part i: solving problems with box constraints, IEEE Trans. Evol. Comput. 18 (4) (2014) 577–601.
[39] Y. Mei, K. Tang, X. Yao, Decomposition-based memetic algorithm for multiobjective capacitated arc routing problem, IEEE Trans. Evol. Comput. 15 (2) (2011) 151–165.
[40] H. Ishibuchi, Y. Setoguchi, H. Masuda, Y. Nojima, Performance of decomposition-based many-objective algorithms strongly depends on pareto front shapes, IEEE Trans. Evol. Comput. 21 (2) (2017) 169–190.
[41] X. Qiu, J.X. Xu, K.C. Tan, H.A. Abbass, Adaptive cross-generation differential evolution operators for multiobjective optimization, IEEE Trans. Evol. Comput. 20 (2) (2016) 232–244.
[42] H. Zhang, X. Zhang, X.Z. Gao, S. Song, Self-organizing multiobjective optimization based on decomposition with neighborhood ensemble, Neurocomputing 173 (2016) 1868–1884.
[43] D. Hadka, P. Reed, Borg: an auto-adaptive many-objective evolutionary computing framework, Evol. Comput. 21 (2) (2013) 231–259.
[44] K. Deb, R.B. Agrawal, Simulated binary crossover for continuous search space, Complex Syst. 9 (2) (1995) 115–148.
[45] J. Brest, S. Greiner, B. Boskovic, M. Mernik, V. Zumer, Self-adapting control parameters in differential evolution: a comparative study on numerical benchmark problems, IEEE Trans. Evol. Comput. 10 (6) (2006) 646–657, https://doi.org/10.1109/TEVC.2006.872133.
[46] S. Dasgupta, S. Das, A. Biswas, A. Abraham, On stability and convergence of the population-dynamics in differential evolution, AI Commun. 22 (1) (2009) 1–20.
[47] Y. Tian, R. Cheng, X. Zhang, F. Cheng, Y. Jin, An indicator based multi-objective evolutionary algorithm with reference point adaptation for better versatility, IEEE Trans. Evol. Comput. 22 (4) (2018) 609–622.
[48] R. Cheng, Y. Jin, M. Olhofer, B. Sendhoff, A reference vector guided evolutionary algorithm for many-objective optimization, IEEE Trans. Evol. Comput. 20 (5) (2016) 773–791.
[49] I. Das, J.E. Dennis, Normal-boundary intersection: a new method for generating the pareto surface in nonlinear multicriteria optimization problems, SIAM J. Optim. 8 (3) (1998) 631–657.
[50] H. Jain, K. Deb, An evolutionary many-objective optimization algorithm using reference-point based nondominated sorting approach, part ii: handling constraints and extending to an adaptive approach, IEEE Trans. Evol. Comput. 18 (4) (2014) 602–622.
[51] S. Jiang, Z. Cai, J. Zhang, Y.-S. Ong, Multiobjective optimization by decomposition with pareto-adaptive weight vectors, in: Natural Computation (ICNC), 2011 Seventh International Conference on, vol. 3, IEEE, 2011, pp. 1260–1264.
[52] Y. Qi, X. Ma, F. Liu, L. Jiao, J. Sun, J. Wu, MOEA/D with adaptive weight adjustment, Evol. Comput. 22 (2) (2014) 231–264.
[53] IEEE Std 754-2008, IEEE Standard for Floating-point Arithmetic, 2008, pp. 1–70, https://doi.org/10.1109/IEEESTD.2008.4610935.
[54] C.A.R. Hoare, Quicksort, Comput. J. 5 (1) (1962) 10–16.
[55] G. Rudolph, A. Agapie, Convergence properties of some multi-objective evolutionary algorithms, in: Evolutionary Computation, 2000. Proceedings of the 2000 Congress on, vol. 2, IEEE, 2000, pp. 1010–1016.
[56] K. Deb, L. Thiele, M. Laumanns, E. Zitzler, Scalable multi-objective optimization test problems, in: Proceedings of the Congress on Evolutionary Computation (CEC-2002), (Honolulu, USA), Proceedings of the Congress on Evolutionary Computation (CEC-2002),(Honolulu, USA), 2002, pp. 825–830.
[57] S. Huband, L. Barone, L. While, P. Hingston, A scalable multi-objective test problem toolkit, in: International Conference on Evolutionary Multi-Criterion Optimization, Springer, 2005, pp. 280–295.
[58] S. Huband, P. Hingston, L. Barone, L. While, A review of multiobjective test problems and a scalable test problem toolkit, Evolut. Comput., IEEE Trans. 10 (5) (2006) 477–506.
[59] Q. Zhang, A. Zhou, S. Zhao, P. N. Suganthan, W. Liu, S. Tiwari, reportMultiobjective Optimization Test Instances for the CEC 2009 Special Session and Competition, University of Essex, Colchester, UK and Nanyang technological University, Singapore, special session on performance assessment of multi-objective optimization algorithms, technical report 264.
[60] M. Pal, S. Bandyopadhyay, Reliability of convergence metric and hypervolume indicator for many-objective optimization, in: Control, Instrumentation, Energy & Communication (CIEC), 2016 2nd International Conference on, IEEE, 2016, pp. 511–515, https://doi.org/10.1109/CIEC.2016.7513806.
[61] Z. He, G.G. Yen, An improved visualization approach in many-objective optimization, in: Evolutionary Computation (CEC), 2016 IEEE Congress on, IEEE, 2016, pp. 1618–1625.
[62] Z. Yang, K. Tang, X. Yao, Self-adaptive differential evolution with neighborhood search, in: Evolutionary Computation, 2008. CEC 2008.(IEEE World Congress on Computational Intelligence). IEEE Congress on, IEEE, 2008, pp. 1110–1116.
[63] G. Wu, R. Mallipeddi, P.N. Suganthan, Ensemble strategies for population-based optimization algorithms – a survey, Swarm Evolut. Comput. (2019), https://doi.org/10.1016/j.swevo.2018.08.015.
[64] W. Khan, Q. Zhang, MOEA/D-DRA with two crossover operators, in: Computational Intelligence (UKCI), 2010 UK Workshop on, IEEE, 2010, pp. 1–6.
[65] S.-Z. Zhao, P.N. Suganthan, Q. Zhang, Decomposition-based multiobjective evolutionary algorithm with an ensemble of neighborhood sizes, IEEE Trans. Evol. Comput. 16 (3) (2012) 442–446.
[66] T. Robič, B. Filipič, DEMO: differential evolution for multiobjective optimization, in: C.A.C. Coello, A.H. Aguirre, E. Zitzler (Eds.), Evolutionary Multi-Criterion Optimization, Springer Berlin Heidelberg, Berlin, Heidelberg, 2005, pp. 520–533.
[67] A.K. Qin, P.N. Suganthan, Self-adaptive differential evolution algorithm for numerical optimization, in: Evolutionary Computation, 2005. The 2005 IEEE Congress on, vol. 2, IEEE, 2005, pp. 1785–1791.
[68] H. Li, K. Deb, Q. Zhang, P. Suganthan, Challenging Novel Many and Multi-Objective Bound Constrained Benchmark Problems, Tech. rep., updated 11 Jan, 2018.
[69] H. Li, K. Deb, Q. Zhang, P.N. Suganthan, L. Chen, Comparison between MOEA/D and NSGA-III on a set of many and multi-objective benchmark problems with challenging difficulties, Swarm Evolut. Comput. 46 (2019) 104–117. https://doi.org/10.1016/j.swevo.2019.02.003.
[70] G. Brown, J. Wyatt, R. Harris, X. Yao, Diversity creation methods: a survey and categorisation, Inf. Fusion 6 (1) (2005) 5–20.
[71] R. Katuwal, P.N. Suganthan, Dropuout and dropconnect based ensemble of random vector functional link neural network, in: IEEE Symposium Symposium Series on Computational Intelligence SSCI 2018, IEEE, 2018, pp. 1772–1778.